EurJIC
European Journal of Inorganic Chemistry

A Journal of ChemPubSoc Europe

Accepted Article

Title: ISOMERIZATION PROCESSES ON ORGANORUTHENIUM COMPLEXES BEARING κ2(P,C)- BIDENTATE LIGANDS GENERATED THROUGH NUCLEOPHILIC ADDITION TO COORDINATED ALKENYL PHOSPHANES

Authors: Isaac García de la Arada, Josefina Díez, Pilar Gamasa, and Elena Lastra

To be cited as: *Eur. J. Inorg. Chem.* 10.1002/ejic.201800895

Link to VoR: http://dx.doi.org/10.1002/ejic.201800895

WILEY-VCH

FULL PAPER WILEY-VCH

ISOMERIZATION PROCESSES ON ORGANORUTHENIUM COMPLEXES BEARING κ^2*P,C*- BIDENTATE LIGANDS GENERATED THROUGH NUCLEOPHILIC ADDITION TO COORDINATED ALKENYL PHOSPHANES

Isaac García de la Arada, Josefina Díez, M. Pilar Gamasa and Elena Lastra*.

Abstract: Nucleophilic attack on complex [RuCl(η^6-$C_{10}H_{14}$){κ^3*P,C,C*-$Ph_2PCH_2CH=CH_2$}][BPh_4] (**2**) takes place, either to the metal or to the coordinated olefin depending on the nucleophile and the reaction conditions. The nucleophilic attack of phosphanes on the coordinated olefin leads diastereoselectively to complexes [RuCl(η^6-$C_{10}H_{14}$){κ^2*P,C*-$Ph_2PCH_2CH(PR_3)CH_2$}]$^+$ bearing κ^2*P,C*-ligands obtained as a racemic mixture of the enantiomers $R_{Ru}Sc/S_{Ru}R_C$. These kinetically stable isomers, undergo an isomerization process leading to the thermodynamically stable products isolated as the diastereoisomer $R_{Ru}R_C/S_{Ru}S_C$. $^{31}P\{^1H\}$ NMR monitoring experiments on the isomerization processes have been carried out.

Introduction

Prochiral alkenes are very useful in enantioselective synthesis.[1] Most of the current examples are based in complexes with enantiopure ligands, however the study of transition metal-fragments bearing a stereogenic centre also plays an important role in activating asymmetric olefins towards the addition of nucleophiles in a stereoselective manner.[2] These metal centres usually have a pseudooctaedral geometry[3] that might induce the selective coordination of the prochiral olefins through one of their enantiotopic faces (see Figure 1). Moreover, providing that rotation around the C=C bond is allowed, two different rotamers can exist for each of the two isomers.

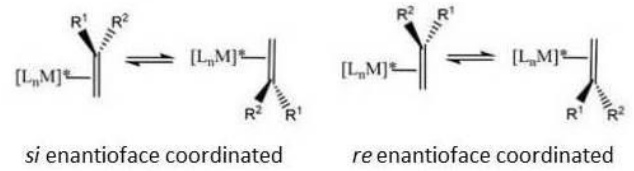

Figure 1. Rotamers and configurational diastereomers generated upon the coordination of prochiral alkenes.

In those cases, the prochiral face selectivity and orientation of olefins are important governing factors that decide the stereochemistry of the product.

A relevant example of nucleophilic attacks of neutral nucleophiles upon coordinated olefins reported in the literature might be the catalytic synthesis of azacyclobutanes.[4] This process occurs through the attack of amines to non-activated olefins, which can happen either in an intermolecular[4,5] or intramolecular way.[6]

On the other hand, hemilabile alkenylphosphane ligands are able to coordinate diastereoselectively to a metal as a chelate κ^3(*P,C,C*), as it has been reported for some examples.[7] This coordination mode has led to interesting reactivities involving the C-C double bond and resulting in one single diastereoisomer.[8]

We have previously reported the synthesis of new half-sandwich ruthenium(II) complexes bearing the hemilabile allyldiisopropylphosphane (ADIP) and explored their behaviour in nucleophilic addition reactions which occur in all cases in a diastereoselective way.[9] In particular, thiolates as anionic S-donor nucleophiles perform two nucleophilic attacks, both to the olefin and the metal centre, giving rise to novel and unprecedented ligands coordinated κ^3(*P,S,C*). On the other hand, tertiary phosphanes as neutral P-donor nucleophiles led to the formation of new ruthenaphosphacycles coordinated κ^2(*P,C*). In this work we have now extended those studies to half-sandwich ruthenium complexes containing the phosphane allyldiphenylphosphane (ADPP) ligand. As a consequence, we are able to stablish a comparison in the hemilability and reactivity of the complexes bearing ADPP and ADIP allylphosphanes, due to their different properties of basicity and size, being the ADIP bulkier and more basic than the ADPP.

Furthermore, we report a closer study to the diastereoselectivity observed in those additions of phosphanes to κ^3*P,C,C* coordinated allylphosphanes, which allows, in some cases, to control the formation of the kinetically stable or the thermodynamically stable diastereoisomer for complexes [RuCl(η^6-$C_{10}H_{14}$){κ^2*P,C*-$R_2PCH_2CH(PR_3)CH_2$}][BPh_4].

Results and Discussion

Synthesis of [$RuCl_2$(η^6-$C_{10}H_{14}$){κ^1*P*-$Ph_2PCH_2CH=CH_2$}] (1) and [RuCl(η^6-$C_{10}H_{14}$){κ^3*P,C,C*-$Ph_2PCH_2CH=CH_2$}][BPh_4] (2). The reaction of the dimeric complex [RuCl(μ-Cl)(η^6-$C_{10}H_{14}$)]$_2$ with a stoichiometric amount of allyldiphenylphosphane (ADPP) in dichloromethane, led to the neutral complex [$RuCl_2$(η^6-$C_{10}H_{14}$){κ^1*P*-$Ph_2PCH_2CH=CH_2$}] (**1**) as an air-stable orange solid. Treatment with $NaBPh_4$ of a methanol suspension of complex **1** resulted in the abstraction of the chloride ligand and coordination of the olefin to the metal center, leading to the cationic complex [RuCl(η^6-$C_{10}H_{14}$){κ^3*P,C,C*-$Ph_2PCH_2CH=CH_2$}][BPh_4] (**2**) which was isolated as an air-stable yellow solid (See Scheme 1).

Dr. I García de la Arada, Prof. J. Díez, Prof. M. P. Gamasa and Prof. E. Lastra
Departamento de Quimica Organica e Inorganica. Universidad de Oviedo, 33006 Oviedo, Principado de Asturias, Spain. Fax: 34-985103446
E-mail for corresponding author: elb@uniovi.es

Supporting information for this article is given via a link at the end of the document.

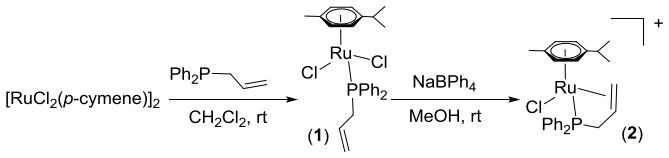

Scheme 1. Synthesis of complexes $[RuCl_2(\eta^6\text{-}C_{10}H_{14})\{\kappa^1P\text{-}Ph_2PCH_2CH{=}CH_2\}]$ (**1**) and $[RuCl(\eta^6\text{-}C_{10}H_{14})\{\kappa^3P,C,C\text{-}Ph_2PCH_2CH{=}CH_2\}][BPh_4]$ (**2**).

Both products were fully characterized by elemental analysis and spectroscopy techniques,[10] which confirm the coordination mode of the allylphosphane as κ^1P for complex **1** and κ^3P,C,C for complex **2**. In particular, IR spectrum for complex **1** shows an absorption corresponding to the non-coordinate C=C double bound at 1629 cm^{-1}, while complex **2** shows the ν(C=C) absorption at 1478 cm^{-1} due to the interaction with the ruthenium. $^{31}P\{^1H\}$ NMR spectra at room temperature also indicate the effect of the olefin coordination, showing the signal for the allylphosphane shifted towards higher field (δ = -63.4 ppm for **2**) with respect to that of the corresponding κ^1P precursor (δ = 24.6 ppm for **1**).

Additionally, the ^1H NMR spectrum of **2** shows $CH{=}CH_2$ resonances which appear at higher fields than those for the olefin in complex **1** because of the π-coordination.

The structure of complex **1** was determined by single crystal X ray diffraction analysis. Suitable crystals were obtained by slow diffusion of hexane into a solution of **1** in CH_2Cl_2. ORTEP type representation of the complex is shown in Figure 2 and selected bond lengths and angles are presented in the caption.

The molecule exhibits a pseudooctahedral three-legged piano-stool geometry with the ruthenium atom bonded to the η^6-*p*-cymene ligand, to the phosphorous atom of the ADPP ligand and to the two chlorine atoms. Bond distances Ru(1)-P(1) (2.341(1) Å) and Ru(1)-Cl (2.419(1) and 2.415(1) Å) are in accordance with those found for ruthenium-phosphane complexes such as $[RuCl_2(PPh_2(CH_2)_3aaaa\eta^6\text{-}C_6H_5)]$[11] (Ru-P: 2.3187 Å; Ru-Cl: 2.4039 and 2.4271 Å), $[RuCl_2(p\text{-}MeC_6H_4Me)(DPVP)]$[12] (Ru-P: 2.3529 Å; Ru-Cl: 2.4065 and 2.4129 Å) or $[RuCl_2(\eta^6\text{-}C_{10}H_{14})(\kappa^1\text{-}(P)\text{-}PPh_2C_4H_5N_2)]$[13] (Ru-P: 2.3523 Å; Ru-Cl: 2.4070 and 2.4320 Å). The C(12)-C(13) bond distance (1.288(7) Å), also agrees with a non-coordinated carbon-carbon double bond.

For complex **2**, the two faces of the alkene coordinated to ruthenium are diastereotopic.[7d, 14] As stated before, the $^{31}P\{^1H\}$ NMR spectrum of complex **2** in CD_2Cl_2 shows one signal (δ = -63.4 ppm) and remains unchanged within a wide range of temperature (-60 to +25 °C). These NMR data agree with a highly diastereoselective generation of the chelate ring $[Ru\{\kappa^3P,C,C\text{-}Ph_2PCH_2CH{=}CH_2\}]$ as reported by us for the complexes $[RuCl(\eta^6\text{-}C_{10}H_{14})\{\kappa^3P,C,C\text{-}iPr_2PCH_2CH{=}CH_2\}][BPh_4]$,[9] $[Ru(\eta^5\text{-}C_9H_7)\{\kappa^3P,C,C\text{-}Ph_2PCH_2CH{=}CH_2\}(PPh_3)][PF_6]$,[7f] and $[Ru(\eta^5\text{-}C_5H_5)\{\kappa^3P,C,C\text{-}Ph_2PCH_2CH{=}CH_2\}(PPh_3)][PF_6]$.[8d]

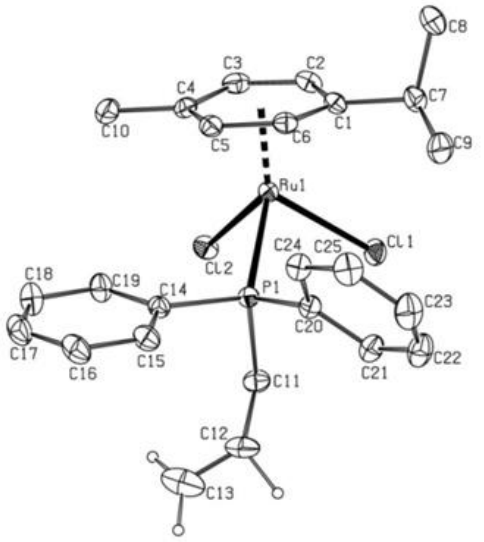

Figure 2. Molecular structure and atom-labeling scheme for the complex $[RuCl_2(\eta^6\text{-}C_{10}H_{14})\{\kappa^1P\text{-}Ph_2PCH_2CH{=}CH_2\}]$ (**1**). Hydrogen atoms except those of the olefin have been omitted for clarity. Non-hydrogen atoms are represented by their 20% probability ellipsoids. C* = centroid of the $\eta^6\text{-}C_{10}H_{14}$ ligand. Selected bond lengths (Å): Ru(1)-Cl(1) = 2.419(1), Ru(1)-Cl(2) = 2.415(1), Ru(1)-P(1) = 2.341(1), P(1)-C(11) = 1.849(3), C(11)-C(12) = 1.487(4), C(12)-C(13) = 1.288(7), Ru(1)-C* = 1.711(1). Selected bond angles (°): Cl(1)-Ru(1)-Cl(2) = 87.23(2), Cl(1)-Ru(1)-P(1) = 84.74(2), Cl(2)-Ru(1)-P(1) = 87.57(2), C*-Ru(1)-P(1) = 130.00(2), C*-Ru(1)-Cl(1) = 127.41(1), C*-Ru(1)-Cl(2) = 125.67(2), C(11)-C(12)-C(13) = 126.20(40).

Complex $[RuCl(\eta^6\text{-}C_{10}H_{14})\{\kappa^3P,C,C\text{-}Ph_2PCH_2CH{=}CH_2\}][BPh_4]$ (**2**) can react with nucleophiles either by ligand substitution on the ruthenium center with displacement of the olefin, or by nucleophilic addition to the coordinated carbon-carbon double bond of the allylphosphane ligand. Competition between the two processes depends principally on the nucleophile.

Nucleophilic attack to the metal center: Synthesis of $[RuCl(\eta^6\text{-}C_{10}H_{14})\{\kappa^1P\text{-}Ph_2PCH_2CH{=}CH_2\}(L)][BPh_4]$ (L = NCMe (3), py (4), $P(OMe)_3$ (5a), $P(OEt)_3$ (5b), $P(OPh)_3$ (5c). When complex $[RuCl(\eta^6\text{-}C_{10}H_{14})\{\kappa^3P,C,C\text{-}Ph_2PCH_2CH{=}CH_2\}][BPh_4]$ (**2**) is dissolved in acetonitrile, complex $[RuCl(\eta^6\text{-}C_{10}H_{14})\{\kappa^1P\text{-}Ph_2PCH_2CH{=}CH_2\}(NCMe)][BPh_4]$ (**3**) is immediately formed. In the same way, the reaction of complex **2** in THF with one equivalent of pyridine or phosphites led instantly to complexes $[RuCl(\eta^6\text{-}C_{10}H_{14})\{\kappa^1P\text{-}Ph_2PCH_2CH{=}CH_2\}(L)][BPh_4]$ (L = py (**4**), $P(OMe)_3$ (**5a**), $P(OEt)_3$ (**5b**), $P(OPh)_3$ (**5c**)) (Scheme 2). The synthesis of these complexes are the result of an olefin-nucleophile exchange and agree with the hemilabile character of the ADPP ligand in complex **2**.

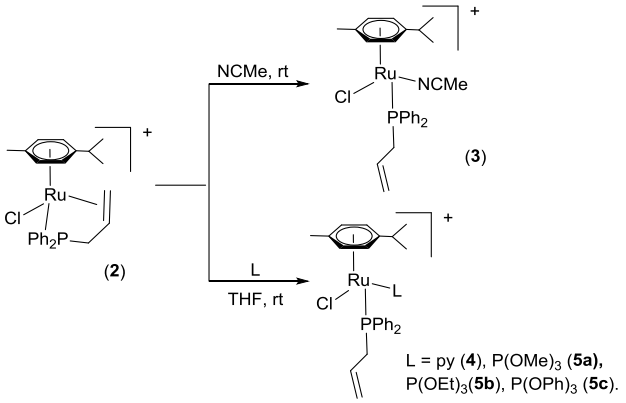

Scheme 2. Synthesis of complexes **3**, **4**, and **5a-c**.

Complexes **3**, **4**, and **5a-c** have been analytically and spectroscopically characterized. In particular, it must be noted that: i) For all complexes, the IR spectra in KBr show the characteristic ν(C=C) absorption in the range 1573-1602 cm^{-1} as expected for non-coordinated C=C double bond. ii) $^{31}P\{^{1}H\}$NMR spectra of complexes **3** and **4** show a singlet at 27.6 (**3**) and 25.7 (**4**), respectively, clearly shifted to lower fields as expected for the ADPP coordinated κ^1P. $^{31}P\{^{1}H\}$NMR spectra of complexes **5a-c** show two doublet signals ($^2J_{PP}$ = 80.2-81.4 Hz), one of them corresponding to the phosphorous atom of the allylphosphane ADPP coordinated κ^1P (29.6-30.6 ppm) and the other corresponding to the phosphorous of the phosphite ligand at low fields (114.9-119.8 ppm). iii) ^{1}H and $^{13}C\{^{1}H\}$NMR spectra show the signals due to the olefin, the p-cymene ring and the phosphite groups (see experimental). iv) Molar conductivity values in acetone for all complexes are in the range expected for electrolytes 1:1.[15]

For this family of complexes we could observe that the ADIP ligand has more tendency to form κ^3P,C,C chelate than the ADPP. Thus, the synthesis of complex **2** requires 12 h of reaction, while the ADIP analogue is completed after 2.5 h. In the same way, complex **3** can be dried at high vacuum, while the ADIP analogue removes the MeCN molecule to coordinate the olefin again. Moreover, opening the chelate with pyridine requires higher temperature for the ADIP than for the ADPP ligand.[9]

Slow diffusion of diethyl ether into a solution of **3** in acetonitrile, and hexane into a solution of **5a** in CH_2Cl_2, allow crystals suitable for single crystal X ray diffraction analysis. ORTEP type representations of the complexes are shown in Figure 3 and selected bond lengths and angles are listed in Table S1 in the Supporting Information.

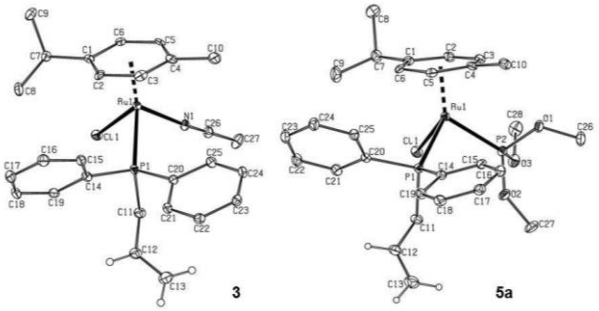

Figure 3. Molecular structure and atom-labeling scheme for the cation of complexes [RuCl(η⁶-$C_{10}H_{14}$){κ¹*P*-$Ph_2PCH_2CH{=}CH_2$}(NCMe)][BPh_4] (**3**) and [RuCl(η⁶-$C_{10}H_{14}$){κ¹*P*-$Ph_2PCH_2CH{=}CH_2$}{$P(OMe)_3$}][BPh_4] (**5a**). Hydrogen atoms (except for the olefin) have been omitted for clarity. Non-hydrogen atoms are represented by their 30% (**3**) or 20% (**5a**) probability ellipsoids.

Nucleophilic attack to the coordinated olefin

Synthesis of ($R_{Ru}S_C/S_{Ru}R_C$)-[RuCl(η⁶-$C_{10}H_{14}$){κ²*P,C*-$Ph_2PCH_2CH(PR_3)CH_2$}][BPh_4] (PR_3 = PMe_3 (6a), PPh_3 (6b), ADPP (6c), ADIP (6d)). When complex **2** reacts with phosphanes, a different behaviour was observed. Thus, the reaction of complex **2** with the phosphanes PMe_3, ADPP and ADIP in THF at room temperature or PPh_3 at -30°C afforded the complexes [RuCl(η⁶-$C_{10}H_{14}$){κ²*P,C*-$Ph_2PCH_2CH(PR_3)CH_2$}][BPh_4] (PR_3 = PMe_3 (**6a**), PPh_3 (**6b**), ADPP (**6c**), ADIP (**6d**)) (Scheme 3).

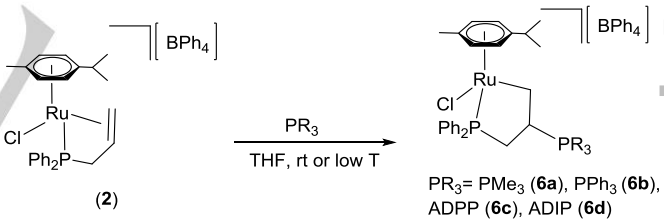

Scheme 3. Synthesis of complexes **6a-d**

Complex **6c** can be also obtained as the chloride salt through the reaction of the dimeric complex [RuCl(μ-Cl)(η⁶-$C_{10}H_{14}$)]$_2$ with an excess of allyldiphenylphosphane (ADPP) in methanol for two hours at room temperature (Scheme 4). The first step for this process must be the formation of the cation of complex **2** in solution and nucleophilic attack of the free ADPP, in the same fashion as it occurs with the analogous product with ADIP ligand.[9]

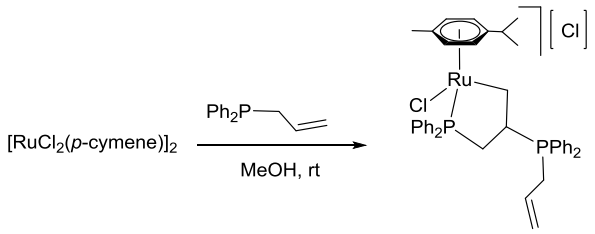

Scheme 4. Synthesis of $[RuCl(\eta^6\text{-}C_{10}H_{14})\{\kappa^2P,C\text{-}Ph_2PCH_2CH(Ph_2PCH_2CH{=}CH_2)CH_2\}][Cl]$.

The complexes **6a-d** are isolated as their tetraphenylborate salts in good yields as yellow stable solids. For all compounds, molar conductivity values in acetone are in the range expected for electrolytes 1:1[15] and the analyses and electrospray mass spectra agree with the proposed stoichiometries.

The complexes have been fully spectroscopically characterized. Significantly, $^{31}P\{^1H\}$ NMR spectra are indicative of the coordination mode of the allylphosphane and the diastereoselectivity of this reaction since these spectra show two doublets ($^3J_{PP}$ = 68.1-85.2 Hz) according with the two different phosphorous atoms in the molecule at δ = 71.7 and 26.6 (**6a**), 72.7 and 26.0 (**6b**), 72.5 and 25.9 ppm (**6c**) and 71.8 and 37.7 (**6d**) ppm for the phosphane and phosphonium moieties, respectively.

The ^1H and $^{13}C\{^1H\}$ NMR spectra also show the signals corresponding to a sole diastereoisomer and agree with the proposed structure (See Experimental).

The structure of complex **6a** was determined by single-crystal X-ray diffraction analysis. Suitable crystals were obtained by slow diffusion of diethyl ether into a solution of compound **6a** in methanol. ORTEP type representation of the complex is shown in Figure 4 and selected bond lengths and angles are presented in the caption.

The most remarkable feature in this pseudooctahedral structure is the presence of the ruthenaphosphacycle with the trimethylphosphonium substituent. The bond distance C(12)-P(2) of 1.817(3) Å is typical of a phosphorous-carbon single bond, and the carbon atoms C(11), C(12), and C(13) in the ruthenaphosphacycle present sp^3 hybridization, as shown by the bond angles around them close to 109°.

The Ru(1)-C(13) bond distance (2.146(3) Å) agree with a ruthenium-carbon single bond and with those found for complex $[RuCl(\eta^6\text{-}C_{10}H_{14})\{\kappa^2P,C\text{-}i Pr_2PCH_2CH(iPr_2PCH_2CH{=}CH_2)CH_2\}][BPh_4]$ of 2.142(2) Å.[9]

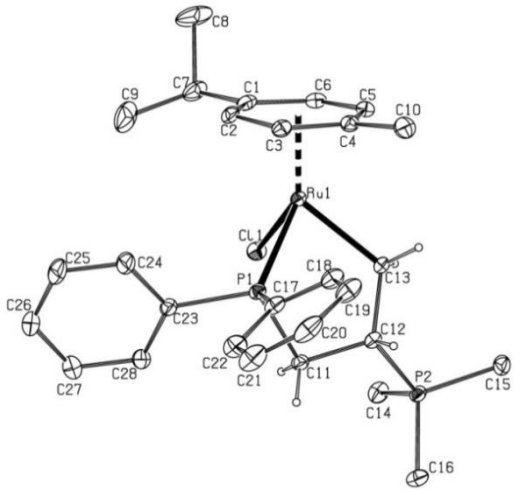

Figure 4. Molecular structure and atom-labeling scheme for the cation of complex $[RuCl(\eta^6\text{-}C_{10}H_{14})\{\kappa^2(P,C)\text{-}Ph_2PCH_2CH(PMe_3)CH_2\}][BPh_4]\cdot MeOH$ (**6a**·MeOH). Hydrogen atoms (except for the ruthenaphosphacycle) have been omitted for clarity. Non-hydrogen atoms are represented by their 10% probability ellipsoids. C* = centroid of the η^6-p-cymene ligand. Selected bond lengths (Å): Ru(1)−Cl(1) = 2.432(1), Ru(1)−P(1) = 2.277(1), Ru(1)−C(13) = 2.146(3), Ru(1)-C* = 1.738(1), P(1)−C(11) = 1.833(3), C(11)−C(12) = 1.532(4), C(12)−C(13) = 1.556(4), C(12)-P(2) = 1.817(3). Selected bond angles (deg): Cl(1)−Ru(1)−P(1) = 84.63(3), Cl(1)-Ru(1)-C(13) = 84.24(8), P(1)-Ru(1)-C(13) = 80.20(8), C*−Ru(1)−Cl(1) = 124.88(3), C*−Ru(1)−P(1) = 135.98(2), C*−Ru(1)−C(13) = 129.21(8), Ru(1)−C(13)−C(12) = 118.69(18), P(2)−C(12)−C(13) = 110.78(19), C(11)−C(12)−C(13) = 113.80(20), P(2)-C(12)-C(11) = 110.34(19).

The formation of complexes **6a-d** is diastereoselective, since only one diastereoisomer is detected by NMR spectroscopy. $^{31}P\{^1H\}$ NMR spectra at low temperature (-60°C) were carried out to discard the existence of dynamic processes for these complexes.

The observed diastereoisomer ($R_{Ru}S_C/S_{Ru}R_C$) is the same as the one obtained for the complex $[RuCl(\eta^6\text{-}C_{10}H_{14})\{\kappa^2P,C\text{-}iPr_2PCH_2CH(iPr_2PCH_2CH{=}CH_2)CH_2\}][Cl]$ as shown in our previous work.[9] This fact can be explained through the diastereoselectivity observed in the formation of the precursor κ^3P,C,C complexes as reported for the analogous complexes $[RuCl(\eta^6\text{-}C_{10}H_{14})\{\kappa^3P,C,C\text{-}iPr_2PCH_2CHCH_2\}][BPh_4]$ which presents the racemic mixture of absolute configuration R_{Ru} and olefin coordination through the *si* enantioface, and S_{Ru} and olefin coordination through the *re* enantioface. Nucleophilic addition to the open face leads to the obtained diastereoisomer as a racemic mixture.

The behavior of phosphanes resulting in a nucleophilic attack over the double bond is in contrast with the reactivity shown by phosphites that lead to an olefin-nucleophile exchange. We assume this difference could be due to the higher relative nucleophilicity of phosphanes towards phosphites.[16]

Synthesis of $RuCl(\eta^6\text{-}C_{10}H_{14})\{\kappa^1P\text{-}Ph_2PCH_2CH{=}CH_2\}(PPh_3)][BPh_4]$ (7). For complex **6b** with the bulky triphenylphosphane, the opening of the cycle and nucleophilic attack of the PPh_3 to the metal center was observed at higher temperatures, resulting in the κ^1P-ADPP derivative

[RuCl(η^6-$C_{10}H_{14}$){κ^1*(P)*-$Ph_2PCH_2CH{=}CH_2$}(PPh_3)][BPh_4] (**7**). This complex can be also obtained by treatment of complex **2** with triphenylphosphane in refluxing THF. For this reaction, the first step must be the quick initial attack of the phosphane to the double bond, giving rise to complex **6b** (Scheme 5) followed by the ring opening, since the reaction of **2** to give complex **6b** takes place at much lower temperature.

Complex **7** shows two doublet signals in the $^{31}P\{^1H\}$ NMR at 19.5 ppm for the PPh_3 and at 23.6 ppm for the ADPP ligand ($^2J_{PP}$ = 52.2 Hz), typical for its κ^1*P* coordination mode. Also the IR, ^1H and $^{13}C\{^1H\}$ NMR agree with the presence of the non-coordinated olefin moiety. Thus, the more relevant spectroscopic data are as follow: i) IR spectrum shows an absorption corresponding to the C=C double bound at 1579 cm^{-1}. ii) olefinic protons appear as two doublets at 4.36 ($^3J_{HH}$ = 16.8 Hz) and 4.63 ppm ($^3J_{HH}$ = 10.4 Hz) for the $=CH_2$ group and a multiplet at 4.71 ppm for the =CH. Iii) the corresponding carbons appear as doublets at 120.5 ppm ($^3J_{CP}$ = 9.9 Hz) and 128.6 ppm ($^2J_{CP}$ = 11.5 Hz) respectively.

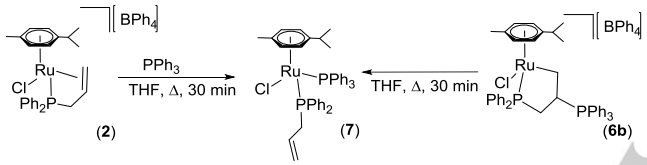

Scheme 5. Synthesis of [RuCl(η^6-$C_{10}H_{14}$){κ^1*(P)*-$Ph_2PCH_2CH{=}CH_2$}(PPh_3)][BPh_4] (**7**).

Finally, the structure was studied by single-crystal X-ray diffraction analysis. Suitable crystals were obtained by slow diffusion of hexane into a solution of **7** in acetone. An ORTEP type representation of the cationic complex is shown in Figure 5, and selected bond lengths and angles are listed in Table S1 in the Supporting Information. Bond distances Ru(1)-P(1) and Ru(2)-P(2) of 2.378(1) and 2.356(1) Å are typical of ruthenium-phosphorous single bonds, while the distance C(12)-C(13) of 1.245(6) Å undoubtedly shows the presence of the non-coordinated olefin. The figure represents the enantiomer with absolute configuration *S* for the metal center, although both enantiomers (*S* and *R*) are present in the crystal as the racemic mixture.

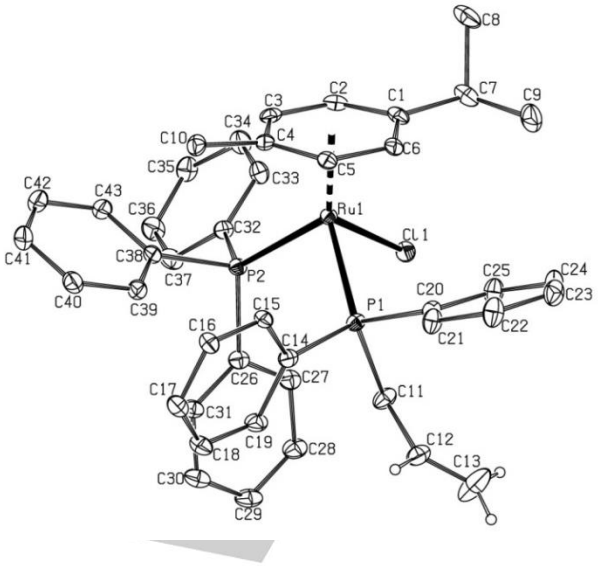

Figure 5. Molecular structure and atom-labeling scheme for the cationic complex [RuCl(η^6-$C_{10}H_{14}$){κ^1*(P)*-$Ph_2PCH_2CH{=}CH_2$}(PPh_3)]$^+$ (**7**). Hydrogen atoms (except for the olefin) have been omitted for clarity. Non-hydrogen atoms are represented by their 20% probability ellipsoids.

Isomerization processes. Synthesis of ($R_{Ru}R_C/S_{Ru}S_C$)-[RuCl(η^6-$C_{10}H_{14}$){κ^2*P,C*-$Ph_2PCH_2CH(PR_3)CH_2$}][BPh_4] (PR_3 = PPh_3 (6b), ADPP (6c)). When the synthesis of complexes **6b** and **6c** were carried out using longer reaction times, a different set of signals appear in the $^{31}P\{^1H\}$ NMR spectra along with those due to complexes **6b** and **6c**. This transformation into the new complexes **6b'** and **6c'** can be completed and they could be isolated and characterized. Their analytical data as well as the ^1H and $^{13}C\{^1H\}$ NMR spectroscopy data are exactly the same than those found for complexes **6b** and **6c**. The only differences were found in the $^{31}P\{^1H\}$ NMR spectra which show two doublets at δ = 66.6 and 25.6 ppm ($^3J_{PP}$ = 74.1 Hz) for complex **6b'** and at δ = 68.0 and 27.4 ppm ($^3J_{PP}$ = 70.5 Hz) for complex **6c'**. These new complexes can be also obtained by stirring at room temperature the isolated complexes **6b** (72.7 and 26.0, $^3J_{PP}$ = 81.4 Hz), and **6c** (72.5 and 25.9, $^3J_{PP}$ = 85.2 Hz) for 2 h or 7 days, respectively.

According to this finding and to the spectroscopic data obtained for the new complexes **6b'** and **6c'**, these can be proposed as the result of the isomerization from the kinetically obtained diasteroisomers ($R_{Ru}S_C/S_{Ru}R_C$) **6b** and **6c** to the thermodynamically more stable ($R_{Ru}R_C/S_{Ru}S_C$) diasteroisomers **6b'** and **6c'**.

For complexes **6a** and **6d** no isomerization was observed and they were found to be stables even in refluxing THF. Based on the chemical shift on the $^{31}P\{^1H\}$ NMR spectra of the phosphorous bonded to the ruthenium (Ru-PPh_2) of these complexes (71.7 (**6a**) and 71.8 (**6d**)), we conclude it is the kinetic product that is formed. These chemical shifts are in agreement with the data obtained for the kinetic products **6b**

(72.7 ppm) and **6c** (72.5 ppm) and different from the values obtained for the thermodynamic products (66.6 ppm for complex **6b'** and 68.0 ppm for complex **6c'**).

Slow diffusion of hexane into a solution of compound **6c'** in dichloromethane allows suitable crystals for X-ray diffraction analysis. Figure 6 shows an ORTEP-type view of the enantiomer with absolute configuration *S* in the ruthenium and *S* for the stereogenic carbon C(12). However, both enantiomers ($S_{Ru}S_C$ and $R_{Ru}R_C$) are present in the crystal in equal proportion, as the crystal belongs to the centric space group $P2_1/c$. Selected bonding data are collected in the caption.

The bond distances and angles found for complex **6c'** are comparable to those obtained for the kinetically stable isomer of complex **6a** and no significant differences can be observed for the two diastereoisomers.

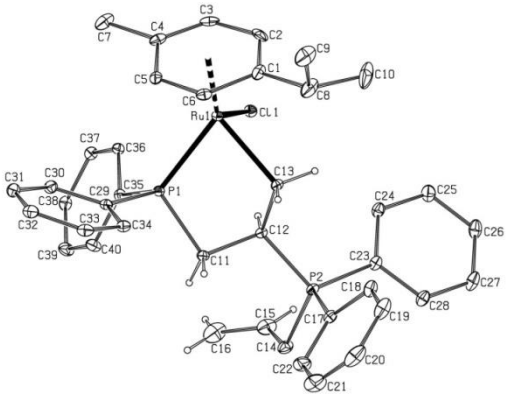

Figure 6. Molecular structure and atom-labeling scheme for the cation of complex [RuCl(η^6-$C_{10}H_{14}$){κ^2(*P,C*)-$Ph_2PCH_2CH(Ph_2PCH_2CH{=}CH_2)CH_2$}][$BPh_4$] (**6c'**). Hydrogen atoms (except for the ruthenaphosphacycle) have been omitted for clarity. Non-hydrogen atoms are represented by their 20% probability ellipsoids. C* = centroid of the η6-p-cymene ligand. Selected bond lengths (Å): Ru(1)−Cl(1) = 2.412(1), Ru(1)−P(1) = 2.285(1), Ru(1)−C(13) = 2.153(2), Ru(1)-C* = 1.725(1), P(1)−C(11) = 1.842(3), C(11)−C(12) = 1.527(3), C(12)−C(13) = 1.531(3), C(12)-P(2) = 1.799(2). Selected bond angles (deg): Cl(1)−Ru(1)−P(1) = 93.18(2), Cl(1)-Ru(1)-C(13) = 82.99(7), P(1)-Ru(1)-C(13) = 79.84(7), C*−Ru(1)−Cl(1) = 123.77(2), C*−Ru(1)−P(1) = 130.31(2), C*−Ru(1)−C(13) = 131.32(6), Ru(1)−C(13)−C(12) = 111.10(16), P(2)−C(12)−C(13) = 114.70(17), C(11)−C(12)−C(13) = 108.40(20), P(2)-C(12)-C(11) = 114.47(17).

On the basis of this finding, the behavior towards phosphanes of the previously reported complex [RuCl(η^6-$C_{10}H_{14}$){κ^3*P,C,C*-*i*$Pr_2PCH_2CH{=}CH_2$}][BPh_4][9] bearing ADIP ligand was reinvestigated through $^{31}P\{^1H\}$ NMR. Thus, the reaction of this complex with phosphanes (PPh_3 (2 min at -30°C), ADPP or ADIP (2 min at rt)) led to the kinetically stable diastereoisomers $R_{Ru}S_C/S_{Ru}R_C$, [RuCl(η^6-$C_{10}H_{14}$){κ^2*P,C*-*i*$Pr_2PCH_2CH(PR_3)CH_2$}][BPh_4][17] but they evolve in solution to the thermodynamically stable diastereoisomers $R_{Ru}R_C/S_{Ru}S_C$. The diastereoisomer $R_{Ru}S_C/S_{Ru}R_C$ was found to be stable for complex [RuCl(η^6-$C_{10}H_{14}$){κ^2*P,C*-*i*$Pr_2PCH_2CH(PMe_3)CH_2$}][BPh_4], at room temperature and under refluxing THF conditions, as reported here for the analogous complex **6a**.

Table 1 shows the $^{31}P\{^1H\}$ NMR data for both diastereoisomers of the complexes bearing ADIP. The thermodynamically stable $R_{Ru}R_C/S_{Ru}S_C$ diasteroisomers were obtained as pure complexes after stirring at room temperature for 30 min (PPh_3), overnight (ADPP) or refluxing overnight (ADIP).

Table 1. $^{31}P\{^1H\}$ NMR data for complexes complexes [RuCl(η^6-$C_{10}H_{14}$){κ^2*P,C*-*i*$Pr_2PCH_2CH(PR_3)CH_2$}][BPh_4] bearing ADIP.[a]

PR_3	$R_{Ru}S_C/S_{Ru}R_C$	$R_{Ru}R_C/S_{Ru}S_C$
PPh_3	85.5 and 25.3 (74.1 Hz)	81.0 and 26.0 (68.0 Hz)
ADPP	86.1 and 24.0 (68.0 Hz)	81.4 and 26.5 (64.4 Hz)
ADIP	86.6 and 36.5 (63,2 Hz)	80.6 and 36.9 (58.3 Hz)

[a] Values in ppm. $^3J_{PP}$ in Hz.

As shown, the isomerization processes depend largely on the size of the phosphonium group and the PR_2 moiety bonded to the metal center. Thus, the complexes with the phosphonium with the smallest cone angle (PMe_3) do not undergo isomerization. However, the complexes with the large PPh_3, evolve readily to the thermodynamically controlled isomer and for complex **6b**, the synthesis must be performed at -30°C. Besides, for the same phosphonium moiety, complexes bearing ADIP isomerize faster than those bearing ADPP.

These isomerization processes have been also detected for rhodium and iridium complexes [MCl(η^5-C_5Me_5){κ^2*(P,C)*-*i*$Pr_2PCH_2CH(PPh_3)CH_2$}][BPh_4].[18]

The mechanism proposed for these rhodium and iridium complexes starts with a β-H elimination to give a metal hydride which would insert into the alkene to give the thermodynamic product. Even when this mechanism can be proposed for our complexes (Scheme 6, pathway A), we cannot rule out the opening of the ruthenaphosphacycle (Scheme 6, pathway B).

In order to get insight into the mechanism of these isomerization processes, a sample of complex **6b** in CD_2Cl_2 was prepared at 233 K and monitorized by $^{31}P\{^1H\}$ NMR spectroscopy (Figure 7). As the temperature was raising up, the isomerization from the kinetic product **6b** to the thermodynamic product **6b´** was observed and the formation of transient species is assessed by the $^{31}P\{^1H\}$ NMR spectra, which show peaks corresponding to complex [RuCl(η^6-$C_{10}H_{14}$){κ^3*P,C,C*-$Ph_2PCH_2CH{=}CH_2$}][BPh_4] (**2**) together with small peaks which can be assigned to complex **7**.

After 4 h at rt, the isomerization is complete and the thermodynamic complex **6b'** appears together with a small amount of ADPP-oxide. On the bases of this finding, the decoordination of the olefin from the metal centre is proposed for the observed isomerization. Furthermore, no hydride signal was observed in the ^1H NMR spectra at any time and allowing discarding pathway A.

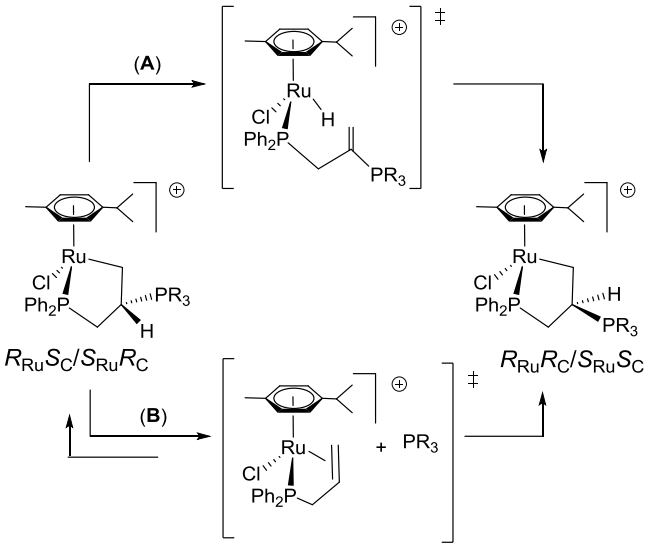

Scheme 6. Plausible pathways for isomerization of complexes 6b and 6c.

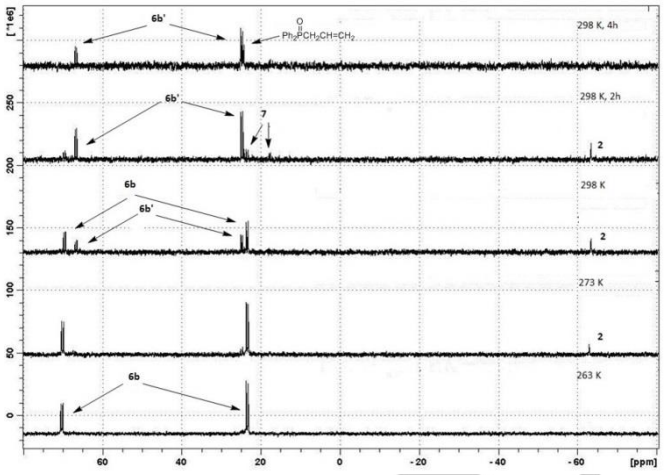

Figure 7. Monitorization of the isomerization process for complex **6b** through $^{31}P\{^{1}H\}$ NMR spectroscopy

In order to understand the thermodynamics of this transformation, the structure of the two diastereoisomers of the complex cations $[RuCl(\eta^6\text{-}C_{10}H_{14})\{\kappa^2P,C\text{-}i Pr_2PCH_2CH(PMe_3)CH_2\}]^+$ and $[RuCl(\eta^6\text{-}C_{10}H_{14})\{\kappa^2P,C\text{-}i Pr_2PCH_2CH(iPr_2PCH_2CH{=}CH_2)CH_2\}]^+$ were investigated theoretically with the Density-functional Theory (DFT) method. The geometry of the two complexes was fully optimized with the B3LYP functional, using the 6-31G* basis set for C, H, P and Cl, and LANL2DZ for Ru. The stationary points located were characterized as minima by calculating the vibrational frequencies. The calculations were carried out with the program Gaussian09.[19]

According to the calculations, the isomerization reactions are spontaneous in the two cases considered. Thus, in the case of $[RuCl(\eta^6\text{-}C_{10}H_{14})\{\kappa^2P,C\text{-}iPr_2PCH_2CH(iPr_2PCH_2CH{=}CH_2)CH_2\}]^+$ complex, the diastereoisomer ($R_{Ru}S_C$), which is formed initially, is predicted to be 5.2 kcal mol^{-1} less stable than the ($R_{Ru}R_C$)

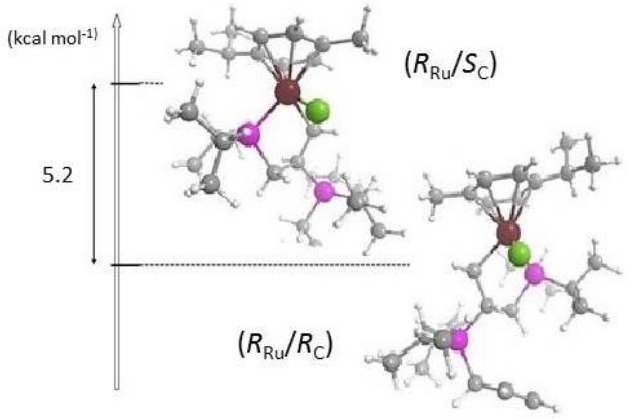

isomer, this compound being the product of thermodynamic control of the reaction (see Figure 8).

Figure 8. Calculations for the cation complex $[RuCl(\eta^6\text{-}C_{10}H_{14})\{\kappa^2P,C\text{-}iPr_2PCH_2CH(iPr_2PCH_2CH{=}CH_2)CH_2\}]^+$

On the other hand, in the case of the complex with the trimethylphosphonium group, which do not experience isomerization, the difference in stability of the two diastereoisomers ($R_{Ru}S_C$) and ($R_{Ru}R_C$) results to be 2.9 kcal mol^{-1}, lower than in the case of the complex previously studied (see Figure 9).

The two isomerization reactions considered are, thus, predicted to be exothermic, but the change in the Gibbs free-energy is higher in the first case. Using the Hammond postulate[20] it can be proposed that the reaction with a lower change in the Gibbs free-energy, could have a higher value of the activation energy. In the present case, this implies that the activation barrier for the isomerization of the ($R_{Ru}S_C$), diastereoisomer of the first complex $[RuCl(\eta^6\text{-}C_{10}H_{14})\{\kappa^2P,C\text{-}iPr_2PCH_2CH(iPr_2PCH_2CH{=}CH_2)CH_2\}]^+$ is lower than in the case of the ($R_{Ru}S_C$) diastereoisomer of the $[RuCl(\eta^6\text{-}C_{10}H_{14})\{\kappa^2P,C\text{-}iPr_2PCH_2CH(PMe_3)CH_2\}]^+$ complex. This could explain that, the isomerization reaction leading to the corresponding product of thermodynamic control of complex $[RuCl(\eta^6\text{-}C_{10}H_{14})\{\kappa^2P,C\text{-}iPr_2PCH_2CH(PMe_3)CH_2\}]^+$, under the current reaction conditions, does not take place.

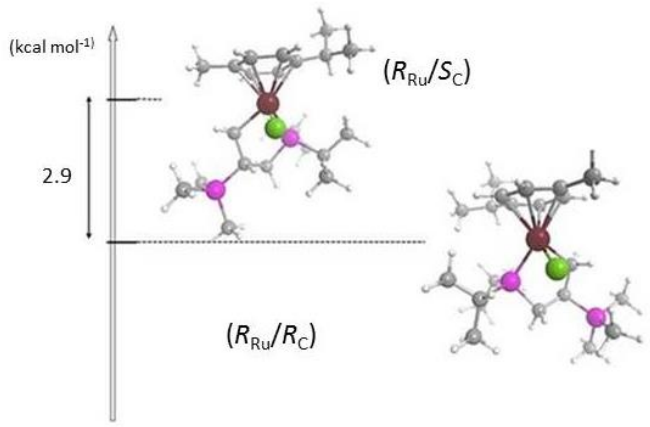

Figure 9. Calculations for the cation complex $[RuCl(\eta^6\text{-}C_{10}H_{14})\{\kappa^2P,C\text{-}i Pr_2PCH_2CH(PMe_3)CH_2\}]^+$

Conclusions

In summary, the nucleophilic attack to the coordinated ADPP ligand in complex $[RuCl(\eta^6\text{-}C_{10}H_{14})\{\kappa^3P,C,C\text{-}Ph_2PCH_2CH{=}CH_2\}]$ (**2**), allows the diastereoselective synthesis of complexes with bidentate κ^2P,C- ligands. The complexes are isolated as the kinetically stable diastereoisomers ($R_{Ru}S_C/S_{Ru}R_C$) which can undergo an isomerization to give the thermodynamically stable diastereoisomers $R_{Ru}R_C/S_{Ru}S_C$. NMR studies in CD_2Cl_2 allow to propose the decoordination of the olefin of the ADPP ligand as the most plausible mechanism for the isomerization processes and DFT calculations shed light on the thermodynamics of this transformation and agree with the experimental results.

The nucleophilic addition to the κ^3P,C,C-alkenylphosphane ligand is competitive with the coordination of the nucleophile to the ruthenium and substitution of the coordinated π-olefin group as observed for N-donor and phosphite ligands.

Experimental Section

All manipulations were performed under an atmosphere of dry nitrogen using vacuum-line and standard Schlenk techniques. All reagents were obtained from commercial suppliers and used without further purification. Solvents were dried by standard methods and distilled under nitrogen before use. Complexes $[RuCl(\mu\text{-}Cl)(\eta^6\text{-}C_{10}H_{14})]_2$,[21] and the phosphane $Ph_2PCH_2CHCH_2$ (ADPP)[22] were prepared by previously reported procedures. Infrared spectra were recorded on a Perkin-Elmer 1720-XFT spectrometer. The C, H and N analyses were carried out with a Perkin-Elmer 240-B and a LECO CHNS-TruSpec microanalyzers. Mass spectra (ESI) were determined with a Bruker Esquire 6000 spectrometer, operating in positive mode and using dichloromethane and methanol solutions. NMR spectra were recorded on Bruker spectrometers AV400 operating at 400.1 (^{1}H), 100.6 (^{13}C) and 162.1 (^{31}P) MHz, AV300 operating at 300.1 (^{1}H), 75.5 (^{13}C) and 121.5 (^{31}P) MHz, and AV600 operating at 600.1 (^{1}H) MHz and 150.9 (^{13}C) MHz. DEPT and bidimensional COSY HH, HSQC and HMBC experiments were carried out for all the compounds. Chemical shifts are reported in parts per million and referenced to TMS or 85% H_3PO_4 as standards. Coupling constants *J* are given in hertzs. Abbreviations used: s, singlet; d, doublet; dd, double doublet; t, triplet; q, quartet; sept, septuplet; m, multiplet; br, broad.

Synthesis of complex $[RuCl_2(\eta^6\text{-}C_{10}H_{14})\{\kappa^1P\text{-}Ph_2PCH_2CH{=}CH_2\}]$ (1). To a solution of the complex $[RuCl(\mu\text{-}Cl)(\eta^6\text{-}C_{10}H_{14})]_2$ (0.5 g, 0.81 mmol) in dichloromethane (15 mL), allyldiphenylphosphane (1.62 mmol, 370 µL) were added. The resulting dark red mixture was stirred at room temperature for 10 minutes. The solution was then evaporated and the orange residue was washed with diethyl ether (3 x 10 mL) and dried under reduced pressure. Yield: 0.82 g (95%). Anal. Calcd for $C_{25}H_{29}Cl_2PRu$: C, 56.4; H, 5.5. Found: C, 56.6; H, 5.7. IR (KBr) ν_{max}/cm^{-1} 1629 (C=C). $^{31}P\{^1H\}$ NMR (121.5 MHz, $CDCl_3$, 20°C): δ 24.6 (s). ^{1}H NMR (400.1 MHz, $CDCl_3$, 20°C): δ 0.82 (6H, d, $^3J_{HH}$ = 7.0 Hz, CH*Me*$_2$), 1.88 (3H, s, Me), 2.50 (1H, sept, $^3J_{HH}$ = 7.0 Hz, C*H*Me$_2$), 3.37 (2H, dd, $^2J_{HP}$ = $^3J_{HH}$ = 8.8 Hz, PC*H*$_2$), 4.61 (1H, d, $^3J_{HH}$ = 16.8 Hz, =CH$_2$), 4.78 (1H, d, $^3J_{HH}$ = 9.6 Hz, =CH$_2$), 5.13, 5.30 (2 x 2H, 2d, $^3J_{HH}$ = 5.6 Hz, *p*-cym), 5.37 (1H, m, =CH), 7.47 (6H, m, Ph), 7.86 (4H, t, $^3J_{HH}$ = 8.0 Hz, Ph). $^{13}C\{^1H\}$ NMR (100.6 MHz, $CDCl_3$, 20°C): δ 17.3 (s, *Me*), 21.3 (s, CH*Me*$_2$), 28.5 (d, $^1J_{CP}$ = 26.7 Hz, P*C*H$_2$), 30.0 (s, *C*HMe$_2$), 85.5 (d, $^2J_{CP}$ = 5.8 Hz, *p*-cym), 90.4 (d, $^2J_{CP}$ = 4.2 Hz, *p*-cym), 94.0, 108.0 (2*s*, *p*-cym), 119.9 (d, $^3J_{CP}$ = 9.3 Hz, =CH$_2$), 128.1 (d, $^2J_{CP}$ = 9.5 Hz, PPh$_2$), 129.5 (d, $^2J_{CP}$ = 12.8 Hz, =CH), 130.6 (d, $^4J_{CP}$ = 1.8 Hz, Ph), 132.1 (d, $^1J_{CP}$ = 42.7 Hz, PPh$_2$), 133.6 (d, $^3J_{CP}$ = 8.4 Hz, PPh$_2$). MS-ESI (m/z): 497 (M - Cl, 100%).

Synthesis of complex $[RuCl(\eta^6\text{-}C_{10}H_{14})\{\kappa^3P,C,C\text{-}Ph_2PCH_2CH{=}CH_2\}][BPh_4]$ (2). A suspension of complex $[RuCl_2(\eta^6\text{-}C_{10}H_{14})\{\kappa^1P\text{-}Ph_2PCH_2CH{=}CH_2\}]$ (**1**) (1 mmol, 547 mg) and $NaBPh_4$ (3 mmol, 1.03 g) in MeOH (20 mL), was stirred at room temperature for 12 h. Solvents were then decanted, the solid residue was extracted with dichloromethane and the resultant solution was filtered through kieselguhr and collected in hexane. Solvents were evaporated and the yellow solid was dried under reduced pressure. Yield: 596 mg (73%). Conductivity (acetone, 20°C): Λ = 109 S cm^2 mol^{-1}. Anal. Calcd for $C_{49}H_{49}BClPRu$: C, 72.10; H, 6.05. Found: C, 71.9; H, 6.1%. IR (KBr) ν_{max}/cm^{-1} 1478 (C=C), 737, 707 (BPh_4). $^{31}P\{^1H\}$ NMR (162.1 MHz, CD_2Cl_2, 20°C): δ -63.4 (s). ^{1}H NMR (400.1 MHz, CD_2Cl_2, 20°C): δ 1.24 (6H, d, $^3J_{HH}$ = 6.8 Hz, CH*Me*$_2$), 1.37 (3H, s, Me), 2.39 (1H, sept, $^3J_{HH}$ = 6.8 Hz, C*H*Me$_2$), 3.05, 3.98 (2 x 1H, 2m, PCH$_2$), 4.24 (1H, d, $^3J_{HH}$ = 13.6 Hz, =CH$_2$), 4.50 (1H, m, =CH), 4.68 (1H, dd, $^2J_{HH}$ = $^3J_{HH}$ = 6.0 Hz, =CH$_2$), 4.97, 5.76 (2 x 1H, 2d, $^3J_{HH}$ = 5.2 Hz, *p*-cym), 5.52, 5.84 (2 x 1H, 2d, $^3J_{HH}$ = 6.0 Hz, *p*-cym), 6.91 (4H, t, $^3J_{HH}$ = 7.2 Hz, BPh_4), 7.05 (8H, t, $^3J_{HH}$ = 7.2 Hz, BPh_4), 7.32 (8H, br s, BPh_4), 7.49 – 7.66 (10H, m, PPh$_2$). MS-ESI (m/z) 497 (M$^+$, 100%), 461 (M - Cl, 10).

Synthesis of complex $[RuCl(\eta^6\text{-}C_{10}H_{14})(MeCN)\{\kappa^1P\text{-}Ph_2PCH_2CH{=}CH_2\}][BPh_4]$ (3). Complex $[RuCl(\eta^6\text{-}C_{10}H_{14})\{\kappa^3P,C,\text{-}Ph_2PCH_2CH{=}CH_2\}][BPh_4]$ (**2**) (0.25 mmol, 200 mg) was dissolved in the minimum volume of acetonitrile. The addition of diethyl ether (2mL) and hexane (15mL) afforded a yellow precipitate. Solvents were decanted and the solid residue dried under reduced pressure. Yield: 157 mg (75%). Anal. Calcd for $C_{51}H_{52}BClNPRu$: C, 71.45; H, 6.1; N, 1.6. Found: C, 71.6; H, 6.2; N, 1.55%. Conductivity (acetone, 20°C): Λ = 106 S cm^2 mol^{-1}. IR (KBr) ν_{max}/cm^{-1} 2362 (C≡N), 1579 (C=C), 737, 707 (BPh_4). $^{31}P\{^1H\}$ NMR (121.5 MHz, CD_3CN, 20°C): δ 27.6 (s). ^{1}H NMR (600.1 MHz, CD_3CN, 20°C): δ 0.92 (6H, d, $^3J_{HH}$ = 6.6 Hz, CH*Me*$_2$), 1.88 (3H, s, Me), 2.14 (3H, s, CH_3CN), 2.30 (1H, sept, $^3J_{HH}$ = 6.6 Hz, C*H*Me$_2$), 3.17, 3.36 (2 x 1H, 2m, PCH$_2$), 4.79 (1H, dd, $^2J_{HH}$ = 1.8 Hz, $^3J_{HH}$ = 16.8 Hz, =CH$_2$), 4.91 (1H, dd, $^2J_{HH}$ = 1.8 Hz, $^3J_{HH}$ = 10.2 Hz, =CH$_2$), 5.35 (1H, d, $^3J_{HH}$ = 6.0 Hz, *p*-cym), 5.42 (1H, m, =CH), 5.51 (1H, d, $^3J_{HH}$ = 6.0 Hz, *p*-cym), 5.54 (2H, d, $^3J_{HH}$ =

6.0 Hz, *p*-cym), 6.83 (4H, t, $^3J_{HH}$ = 7.2 Hz, BPh_4), 6.98 (8H, t, $^3J_{HH}$ = 7.8 Hz, BPh_4), 7.27 (8H, m, BPh_4), 7.54 (4H, m, PPh_2), 7.59, 7.69, 7.75 (3 x 2H, 3m, PPh_2). $^{13}C\{^1H\}$ NMR (150.9 MHz, CD_3CN, 20°C): δ 1.4 (s, *C*H_3CN), 18.0 (s, Me), 21.7, 21.8 (s, CH*Me*$_2$), 31.4 (s, C-*C*HMe$_2$), 32.0 (d, $^1J_{CP}$ = 27.3 Hz, PCH_2), 89.5 (d, $^2J_{CP}$ = 4.7 Hz, *p*-cym), 90.1 (d, $^2J_{CP}$ = 4.2 Hz, *p*-cym), 91.3, 95.2, 100.4, 111.6 (4*s*, *p*-cym), 121.0 (d, $^3J_{CP}$ = 10.0 Hz, =CH_2), 122.7, 126.6 (2*s*, BPh_4), 129.3 (s, CH_3*C*N), 129.6 (d, $^2J_{CP}$ = 10.3 Hz, PPh_2), 129.7 (d, $^2J_{CP}$ = 10.2 Hz, PPh_2), 130.0 (d, $^2J_{CP}$ = 11.0 Hz, =CH), 130.4 (d, $^1J_{CP}$ = 48.6 Hz, PPh_2), 131.7 (d, $^1J_{CP}$ = 45.9 Hz, PPh_2), 132.4 (s, PPh_2), 134.1 (d, $^3J_{CP}$ = 8.7 Hz, PPh_2), 134.3 (d, $^3J_{CP}$ = 9.2 Hz, PPh_2), 136.7 (*s*, BPh_4), 164.8 (q, J_{C11B} = 45.3 Hz, BPh_4). MS-ESI (m/z): 497 (M - MeCN, 32%), 463 (M - MeCN - Cl, 100).

Synthesis of complex [RuCl(η^6-$C_{10}H_{14}$)(py){κ^1*P*-$Ph_2PCH_2CH=CH_2$}][BPh_4] (4). To a solution of the complex [RuCl(η^6-$C_{10}H_{14}$){κ^3*P,C,C*-$Ph_2PCH_2CH=CH_2$}][BPh_4] (**2**) (0.1 mmol, 81.6 mg) in THF (10 mL), 1 equivalent of pyridine (0.1 mmol, 8 µl) was added and the mixture was stirred for 5 minutes at reflux temperature. The addition of hexane (50 mL) affords a yellow precipitate which was washed with hexane (3 x 10 mL) and dried under reduced pressure. Yield: 64 mg (72%). Anal. Calcd for $C_{54}H_{54}BClNPRu$: C, 72.4; H, 6.1; N, 1.6. Found: C, 72.5; H, 6.1; N, 1.5%. Conductivity (acetone, 20°C): Λ = 143 S cm^2 mol^{-1}. IR (KBr) ν_{max}/cm^{-1} 1602 (C=C), 733, 703 (BPh_4). $^{31}P\{^1H\}$ NMR (162.1 MHz, CD_2Cl_2, 20°C): δ 25.7 (s). ^1H NMR (400.1 MHz, CD_2Cl_2, 20°C): δ 1.04, 1.11 (2 x 3H, 2d, $^3J_{HH}$ = 6.8 Hz, CH*Me*$_2$), 1.60 (3H, s, Me), 2.28 (1H, sept, $^3J_{HH}$ = 6.8 Hz, C*H*Me$_2$), 2.92, 3.18 (2 x 1H, 2m, PC*H*$_2$), 4.80 (d, $^3J_{HH}$ = 16.8 Hz, 1H, =CH_2), 4.90 (1H, d, $^3J_{HH}$ = 10.0 Hz, =CH_2), 5.16 (1H, d, $^3J_{HH}$ = 6.0 Hz, *p*-cym), 5.24 – 5.36 (4H, m, =CH, *p*-cym), 6.89 (4H, t, $^3J_{HH}$ = 7.2 Hz, BPh_4), 7.03 (8H, t, $^3J_{HH}$ = 7.2 Hz, BPh_4), 7.25 (2H, t, $^3J_{HH}$ = 6.8 Hz, py), 7.33 – 7.80 (19H, m, PPh_2, BPh_4, py), 8.64 (2H, d, $^3J_{HH}$ = 5.6 Hz, py). $^{13}C\{^1H\}$ NMR (100.6 MHz, CD_2Cl_2, 20°C): δ 17.2 (s, Me), 21.4, 21.8 (2*s*, CH*Me*$_2$), 30.6 (s, C-*C*HMe$_2$), 30.9 (d, $^1J_{CP}$ = 27.2 Hz, PCH_2), 86.3, 88.3, 90.4, 91.1, 99.9, 113.0 (6*s*, *p*-cym), 120.8 (d, $^3J_{CP}$ = 9.9 Hz, =CH_2), 121.7, 125.6 (2*s*, BPh_4), 126.0 (s, py), 128.4 (d, $^2J_{CP}$ = 11.5 Hz, =CH), 127.0 – 132.0 (PPh_2), 135.9 (s, BPh_4), 139.4, 155.8 (2*s*, py), 164.1 (q, J_{C11B} = 50.3 Hz, BPh_4). MS-ESI (m/z): 577 (M - py, 100%), 461 (M - py - Cl, 20).

Synthesis of complexes [RuCl(η^6-$C_{10}H_{14}$){κ^1*P*-$Ph_2PCH_2CH=CH_2$}{$P(OR)_3$}][BPh_4] (R = Me (5a), Et (5b), Ph (5c)). To a solution of complex [RuCl(η^6-$C_{10}H_{14}$){κ^3*P,C,C*-$Ph_2PCH_2CH=CH_2$}][BPh_4] (**2**) (0.05 mmol, 40.8 mg) in THF (8 mL), 1 equivalent of the correspondent phosphite $P(OR)_3$ was added and the mixture was stirred at room temperature for 2 minutes. The solution was then concentrated under vacuum to a volume of approx. 1 mL. Addition of hexane (20 mL) afforded a yellow precipitate. Solvents were decanted and the solid was washed with hexane (2 x 10 mL) and dried under reduced pressure. The complexes can be recrystallized from dichloromethane/ diethyl ether if required. R = Me (**5a**): Yield: 28 mg (60%). Anal. Calcd for $C_{52}H_{58}BClO_3P_2Ru$: C, 66.4; H, 6.2. Found: C, 66.7; H, 6.3%. Conductivity (acetone, 20°C): Λ= 126 S cm^2 mol^{-1}. IR (KBr) ν_{max}/cm^{-1} 1578 (C=C), 733, 702 (BPh_4). $^{31}P\{^1H\}$ NMR (121.5 MHz, CD_2Cl_2, 20°C): δ 30.4 (d, $^2J_{PP}$ = 81.4 Hz, ADPP), 119.8 (d, $^2J_{PP}$ = 81.4 Hz, $P(OMe)_3$). ^1H NMR (400.1 MHz, CD_2Cl_2, 20°C): δ 0.90, 1.09 (2 x 3H, 2d, $^3J_{HH}$ = 6.8 Hz, CH*Me*$_2$), 1.78 (3H, s, Me), 2.53 (1H, sept, $^3J_{HH}$ = 6.8 Hz, C*H*Me$_2$), 3.00, 3.66 (2 x 1H, 2m, PCH_2), 3.86 (9H, d, $^3J_{HP}$ = 11.2 Hz, $P(OMe)_3$), 4.80 (1H, d, $^3J_{HH}$ = 16.8 Hz, =CH_2), 4.98 (2H, m, =CH_2, *p*-cym), 5.27 (1H, m, *p*-cym), 5.42 (1H, m, =CH), 5.50, 5.89 (2 x 1H, 2d, $^3J_{HH}$ = 6.0 Hz, *p*-cym), 6.90 (4H, t, $^3J_{HH}$ = 7.2 Hz, BPh_4), 7.05 (8H, t, $^3J_{HH}$ = 7.2 Hz, BPh_4), 7.34 (8H, m, BPh_4), 7.55 –7.77 (10H, m, PPh_2). $^{13}C\{^1H\}$ NMR (100.6 MHz, $CDCl_3$, 20°C): δ 17.5 (s, Me), 20.0, 22.0 (2*s*, CH*Me*$_2$), 30.9 (s, *C*HMe$_2$), 31.3 (d, $^1J_{CP}$ = 28.4 Hz, PCH_2), 55.5 (d, $^2J_{CP}$ = 9.5 Hz, $P(OMe)_3$), 88.4 (d, $^2J_{CP}$ = 8.2 Hz, *p*-cym), 95.1 (d, $^2J_{CP}$ = 11.8 Hz, *p*-cym), 95.4, 100.1, 101.5 (3*s*, *p*-cym) 120.9 (d, $^3J_{CP}$ = 10.7 Hz, =CH_2), 121.7, 125.6 (2*s*, BPh_4), 125.6 (s, *p*-cym), 129.0 (d, $^2J_{CP}$ = 11.8 Hz, =CH), 128.3 – 134.0 (PPh_2), 135.9, (*s*, BPh_4), 164.1 (q, J_{C11B} = 50.3 Hz, BPh_4).. MS-ESI (m/z): 621 (M - $P(OMe)_3$, 100%). R = Et (**5b**): Yield: 33 mg (66%). Anal. Calcd for $C_{55}H_{64}BClO_3P_2Ru$: C, 67.2; H, 6.6. Found: C, 67.3; H, 6.55%. Conductivity (acetone, 20°C): Λ= 138 S cm^2 mol^{-1}. IR (KBr) ν_{max}/cm^{-1} 1580 (C=C), 733, 704 (BPh_4). $^{31}P\{^1H\}$ NMR (121.5 MHz, $CDCl_3$, 20°C): δ 30.6 (d, $^2J_{PP}$ = 80.2 Hz, ADPP), 115.6 (d, $^2J_{PP}$ = 80.2 Hz, $P(OEt)_3$). ^1H NMR (400.1 MHz, $CDCl_3$, 20°C): δ 0.78, 1.08 (2 x 3H, 2d, $^3J_{HH}$ = 6.8 Hz, CH*Me*$_2$), 1.30 (9H, t, $^3J_{HH}$ = 7.2 Hz, CH_2CH_3), 1.49 (3H, s, C-Me), 2.44 (1H, sept, $^3J_{HH}$ = 6.8 Hz, C*H*Me$_2$), 2.86, 3.64 (2 x 1H, 2m, PCH_2), 4.14 (6H, m, C*H*$_2$CH$_3$), 4.50 (1H, d, $^3J_{HH}$ = 6.0 Hz, *p*-cym), 4.71 (1H, dd, $^2J_{HH}$ = 2.8 Hz, $^3J_{HH}$ = 17.2 Hz, =CH_2), 4.96 (2H, m, =CH_2, *p*-cym), 5.29 (1H, d, $^3J_{HH}$ = 6.0 Hz, *p*-cym), 5.40 (1H, m, =CH), 5.60 (1H, m, *p*-cym), 6.85 (4H, t, $^3J_{HH}$ = 7.2 Hz, BPh_4), 6.97 (8H, t, $^3J_{HH}$ = 7.2 Hz, BPh_4), 7.34 (8H, m, BPh_4), 7.35 - 7.63 (10H, m, PPh_2). $^{13}C\{^1H\}$ NMR (100.6 MHz, $CDCl_3$, 20°C): δ 16.1 (d, $^3J_{CP}$ = 6.2 Hz, CH_2*C*H$_3$), 17.4 (s, Me), 19.6, 22.6 (2*s*, CH*Me*$_2$), 30.7 (d, $^1J_{CP}$ = 30.5 Hz, PCH_2), 30.9 (s, *C*HMe$_2$), 64.7 (d, $^2J_{CP}$ = 9.5 Hz, *C*H_2CH$_3$), 87.8, 94.7, 94.9, 99.1, 100.1 (5*s*, *p*-cym), 121.0 (d, $^3J_{CP}$ = 10.4 Hz, =CH_2), 121.7, 125.5 (2*s*, BPh_4), 128.9 (d, $^2J_{CP}$ = 9.9 Hz, =CH), 129.5 (s, *p*-cym), 128.0 – 134.6 (PPh_2), 136.3 (s, BPh_4), 164.1 (q, J_{C11B} = 50.3 Hz, BPh_4). MS-ESI (m/z): 663 (M$^+$, 100%), 360 (M – $P(OEt)_3$ – *p*-cym, 55). R = Ph (**5c**): Yield: 38 mg (68%). Anal. Calcd for $C_{67}H_{64}BClO_3P_2Ru$: C, 71.4; H, 5.7. Found: C, 70.9; H, 5.3%. Conductivity (acetone, 20°C): Λ= 134 S cm^2 mol^{-1}. IR (KBr) ν_{max}/cm^{-1} 1587 (C=C), 734, 705 (BPh_4). $^{31}P\{^1H\}$ NMR (121.5 MHz, $CDCl_3$, 20°C): δ 29.6 (d, $^2J_{PP}$ = 80.2 Hz, ADPP), 114.9 (d, $^2J_{PP}$ = 80.2 Hz, $P(OPh)_3$). ^1H NMR (400.1 MHz, $CDCl_3$, 20°C): δ 0.85, 0.95 (2 x 3H, 2d, $^3J_{HH}$ = 6.8 Hz, CH*Me*$_2$), 1.42 (3H, s, Me), 2.23 (1H, sept, $^3J_{HH}$ = 6.8 Hz, CH*Me*$_2$), 2.87, 3.74 (2 x 1H, 2m, PCH_2), 3.97 (1H, d, $^3J_{HH}$ = 6.0 Hz, *p*-cym), 4.35, 5.04, 5.80 (3 x 1H, 3s, br, *p*-cym), 4.55 (1H, d, $^3J_{HH}$ = 15.2 Hz, =CH_2), 4.85 (1H, d, $^3J_{HH}$ = 8.8 Hz, =CH_2), 5.29 (1H, m, =CH), 6.81 (4H, t, $^3J_{HH}$ = 7.2 Hz, BPh_4), 7.90 (8H, t, $^3J_{HH}$ = 7.2 Hz, BPh_4), 7.04 – 7-.74 (33H, m, BPh_4, PPh_2, $P(OPh)_3$). $^{13}C\{^1H\}$ NMR (100.6 MHz, $CDCl_3$, 20°C): δ 17.4 (s, Me), 19.9, 21.8 (2*s*, CH*Me*$_2$), 30.7 (d, $^1J_{CP}$ = 28.7 Hz, PCH_2), 31.2 (s, *C*HMe$_2$), 85.8 (d, $^2J_{CP}$ = 8.6 Hz, *p*-cym), 93.6 (d, $^2J_{CP}$ = 14.4 Hz, *p*-cym), 98.3, 98.9, 99.1 (3*s*, *p*-cym), 121.5 (d, $^3J_{CP}$ = 10.0 Hz, =CH_2), 121.7, 125.4 (2*s*, BPh_4), 128.4 (d, $^2J_{CP}$ = 11.8 Hz, =CH), 132.7 (s, *p*-cym), 136.3 (s, BPh_4), 121.3 – 134.4 (PPh_2, $P(OPh)_3$), 151.0 (d, $^3J_{CP}$ = 13.5 Hz, $P(OPh)_3$), 164.1 (q, J_{C11B} = 50.3 Hz, BPh_4). MS-ESI (m/z): 807 (M$^+$, 100%).

Synthesis of complexes (*R*$_{Ru}$*S*$_C$/*S*$_{Ru}$*R*$_C$)-[RuCl(η^6-$C_{10}H_{14}$){κ^2*(P,C)*-$Ph_2PCH_2CH(PR_3)CH_2$}][BPh_4] (PR_3 = PMe_3 (6a), PPh_3 (6b), ADPP (6c), ADIP (6d)). To a solution of complex [RuCl(η^6-$C_{10}H_{14}$){κ^3*P,C,C*-$Ph_2PCH_2CH=CH_2$}][BPh_4] (**2**) (0.05 mmol, 40.8 mg) in THF (8 mL), 1 equivalent of the correspondent PR_3 was added (0.05 mmol, 4.5 µl, PMe_3; 13.1 mg, PPh_3, 11 µl , ADPP; 8 µl, ADIP) and the mixture is stirred for 2 minutes at room temperature (PMe_3, ADPP and ADIP) or -30°C (PPh_3). The solution was then concentrated under vacuum to a volume of approx. 1 mL. Addition of diethyl ether (**6a, 6b**) or hexane (**6c, 6d**) (20 mL) afforded a yellow precipitate. Solvents were decanted and the solid was washed with diethyl ether (**6a, 6b**) or hexane (**6c, 6d**) (2 x 10 mL) and dried under reduced pressure. PR_3 = PMe_3 (**6a**): Yield:31 mg (69%). Anal. Calcd for $C_{52}H_{58}BClP_2Ru$: C, 70.00; H, 6.55. Found: C, 69.9; H, 6.6%. Conductivity (acetone, 20°C): Λ = 142 S cm^2 mol^{-1}. IR (KBr) ν_{max}/cm^{-1} 732, 704 (BPh_4). $^{31}P\{^1H\}$ NMR (121.5 MHz, CD_2Cl_2, 20°C): δ 71.7 (d, $^3J_{PP}$ = 71.3 Hz, Ru-PPh_2), 26.6 (d, $^3J_{PP}$ = 71.3 Hz, PMe_3). ^1H NMR (400.1 MHz, CD_2Cl_2, 20°C): δ 0.99, 1.16 (2 x 3H, 2d, $^3J_{HH}$ = 6.8 Hz, CH*Me*$_2$), 1.34 (9H, d, $^2J_{HP}$ = 13.2 Hz, PMe_3), 1.98 (3H, s, Me), 2.19 - 2.40 (4H, m, Ru-P*C*H_2, Ru-*C*H_2, *CH*P), 2.51 (1H, sept, $^3J_{HH}$ = 6.8 Hz, C*H*Me$_2$), 3.03 (1H, m, Ru-*C*H_2), 4.91, 5.02, 5.31, 5.51 (4 x 1H, 4d, $^3J_{HH}$ = 6.0 Hz, *p*-cym) 6.90 (4H, t, $^3J_{HH}$ = 7.2 Hz, BPh_4), 7.06 (8H, t, $^3J_{HH}$ = 7.6 Hz, BPh_4) 7.18 - 7.78 (18H, m, PPh_2, BPh_4). $^{13}C\{^1H\}$ NMR (100.6 MHz, CD_2Cl_2, 20°C): δ 7.1 (d, $^1J_{CP}$ = 55.0 Hz, PMe_3), 15.4 (m, Ru-CH_2), 17.9 (s, Me), 22.1, 22.2 (2*s*, CH*Me*$_2$), 30.7 (s, *C*HMe$_2$), 33.4 (d, $^1J_{CP}$ = 28.8 Hz, Ru-

PCH_2), 34.9 (m, *C*HP), 87.0, 87.3, 88.9, 89.3, 100.2, 110.6 (6*s*, *p*-cym), 121.8, 125.7 (2*s*, BPh_4), 128.2 – 134.0 (PPh_2), 136.0 (s, BPh_4), 164.1 (q, J_{C11B} = 60.4 Hz, BPh_4). MS-ESI (m/z): 573 (M^+, 100%). PR_3 = PPh_3 (**6b**): Yield: 29 mg (53%). Anal. Calcd for $C_{67}H_{64}BClP_2Ru$: C, 74.6; H, 6.0. Found: C, 74.5; H, 6.0%. Conductivity (acetone, 20°C): Λ = 132 S cm^2 mol^{-1}. IR (KBr) ν_{max}/cm^{-1} 732, 704 (BPh_4). $^{31}P\{^1H\}$ NMR (121.5 MHz, CD_2Cl_2, 20°C): δ 72.7 (d, $^3J_{PP}$ = 81.4 Hz, Ru-PPh_2), 26.0 (d, $^3J_{PP}$ = 81.4 Hz, PPh_3). ^1H NMR (400.1 MHz, CD_2Cl_2, 20°C): δ 1.11, 1.17 (2 x 3H, 2d, $^3J_{HH}$ = 6.8 Hz, CH*Me*$_2$) 1.85 (3H, s, Me), 1.97 (2H, m, Ru-PC*H*$_2$, Ru-C*H*$_2$), 2.48 (1H, sept, $^3J_{HH}$ = 6.8 Hz, *C*HMe$_2$), 2.88 (1H, m, Ru-PC*H*$_2$), 3.55 (1H, m, Ru-C*H*$_2$), 4.44 (1H, m, *CH*P), 4.53, 4.68, 4.92, 5.26 (4 x 1H, 4d, $^3J_{HH}$ = 6.0 Hz, *p*-cym), 6.89 (4H, t, $^3J_{HH}$ = 7.2 Hz, BPh_4), 7.04 (8H, t, $^3J_{HH}$ = 7.6 Hz, BPh_4) 6.64 - 7.90 (33H, m, PPh, BPh_4). $^{13}C\{^1H\}$ NMR (100.6 MHz, CD_2Cl_2, 20°C): δ 16.8 (m, Ru-CH_2), 17.6 (s, Me), 21.7, 22.9 (2*s*, CH*Me*$_2$), 30.6(s, *C*HMe$_2$), 32.1 (d, $^1J_{CP}$ = 33.0 Hz, Ru-PCH_2), 32.5 (m, *C*HP), 86.7, 87.6, 88.5, 88.7, 100.8, 111.4 (6*s*, *p*-cym), 121.7, 125.6 (2*s*, BPh_4), 128.6 – 135.2 (PPh), 135.9 (s, BPh_4), 164.3 (q, J_{C11B} = 49.5 Hz, BPh_4). 163.3, 163.8, 164.2, 164.8 MS-ESI (m/z): 759 (M^+, 100%), 497 (M - PPh_3^+, 82). PR_3 = ADPP (**6c**): Yield: 42 mg (81%). Anal. Calcd for $C_{64}H_{64}BClP_2Ru$: C, 73.7; H, 6.2. Found: C, 73.9; H, 6.1%. Conductivity (acetone, 20°C): Λ = 136 S cm^2 mol^{-1}. IR (KBr) ν_{max}/cm^{-1} 1579 (C=C), 733, 704 (BPh_4). $^{31}P\{^1H\}$ NMR (162.1 MHz, $CDCl_3$, 20°C): δ 72.5 (d, $^3J_{PP}$ = 85.2 Hz, Ru-PPh_2), 25.9 (d, $^3J_{PP}$ = 85.2 Hz, CH-PPh_2). ^1H NMR (400.1 MHz, CD_2Cl_2, 20°C): δ 1.15, 1.23 (2 x 3H, 2d, $^3J_{HH}$ = 6.8 Hz, CH*Me*$_2$), 1.90 – 2.08 (2H, m, Ru-PC*H*$_2$, Ru-C*H*$_2$), 2.12 (3H, s, Me), 2.79 (2H, m, C*H*Me$_2$, Ru-PC*H*$_2$), 3.60 (1H, m, Ru-C*H*$_2$), 4.43 (1H, m, PC*H*$_2$-CH=), 4.57 (1H, m, C*H*P), 4.86 (1H, m, PC*H*$_2$-CH=), 4.93, 5.01 (2 x 1H, 2d, $^3J_{HH}$ = 5.6 Hz, *p*-cym), 5.07 (1H, d, $^3J_{HH}$ = 6.0 Hz, *p*-cym), 5.26 (1H, dd, $^2J_{HH}$ = 3.2 Hz, $^3J_{HH}$ = 9.6 Hz, =CH_2), 5.43 (2H, m, =CH_2, *p*-cym), 5.59 (1H, m, =CH), 6.92 (4H, t, $^3J_{HH}$ = 7.2 Hz, BPh_4), 7.06 (8H, t, $^3J_{HH}$ = 7.6 Hz, BPh_4) , 7.36 – 7.72 (28H, m, PPh_2 , BPh_4). $^{13}C\{^1H\}$ NMR (100.6 MHz, CD_2Cl_2, 20°C): δ 18.4 (s, Me), 20.1 (dd, $^2J_{CP}$ = $^3J_{CP}$ = 11.4 Hz, Ru-*C*H$_2$), 21.9, 23.1 (2*s*, CH*Me*$_2$), 27.9 (d, $^1J_{CP}$ = 46.6 Hz, PCH_2-CH=), 30.8 (s, *C*HMe$_2$), 33.9 (d, $^1J_{CP}$ = 25.3 Hz, Ru-PCH_2), 39.0 (m, *C*HP), 85.4, 87.7 (2*s*, *p*-cym), 88.1 (d, $^2J_{CP}$ = 3.8 Hz, *p*-cym), 88.3 (d, $^2J_{CP}$ = 5.2 Hz, *p*-cym), 103.4, 113.9 (2*s*, *p*-cym), 121.7 (s, BPh_4), 123.8 (d, $^3J_{CP}$ = 12.5 Hz, =*C*H$_2$), 125.1 (d, $^2J_{CP}$ = 10.0 Hz, =*C*H), 125.6 (s, BPh_4), 127.9 – 134.5 (PPh_2), 135.2 (s, BPh_4), 164.1 (q, $^1J_{CB}$ = 49.1 Hz, BPh_4). MS-ESI (m/z): 723 (M^+, 100%). PR_3 = ADIP (**6d**): Yield: 34 mg (70%). Anal. Calcd for $C_{58}H_{68}BClP_2Ru$: C, 71.5; H, 7.0. Found: C, 69.4; H, 6.8%. Conductivity (acetone, 20°C): Λ = 131 S cm^2 mol^{-1}. IR (KBr) ν_{max}/cm^{-1} 1579 (C=C), 733, 705 (BPh_4). $^{31}P\{^1H\}$ NMR (162.1 MHz, CD_2Cl_2, 20°C): δ 71.8 (d, $^3J_{PP}$ = 68.1 Hz, Ru-PPh_2), 37.7 (d, $^3J_{PP}$ = 68.1 Hz, CH-P^{i}Pr$_2$). ^1H NMR (400.1 MHz, CD_2Cl_2, -30°C): δ 0.87, 1.10 (2 x 3H, 2*d*, $^3J_{HH}$ = 6.8 Hz, CH*Me*$_2$), 1.26 – 1.41 (12H, m, *Me*$_2$CH-P), 2.07 (3H, s, Me), 2.42 - 2.56 (4H, m, Ru-PC*H*$_2$, C*H*P, C*H*Me$_2$), 2.58 – 2.65 (3H, m, Ru-C*H*$_2$, Me$_2$C*H*-P), 2.94 (2H, dd, $^2J_{HH}$ = 13.8 Hz, $^3J_{HH}$ = 7.6 Hz, PC*H*$_2$-CH=), 3.13 (m, 1H, Ru-C*H*$_2$), 4.88 (1H, br s, *p*-cym), 4.97 (1H, d, $^3J_{HH}$ = 5.9 Hz, *p*-cym), 5.41 – 5.47 (3H, m, =CH_2, *p*-cym), 5.54 (1H, d, $^3J_{HH}$ = 5.9 Hz, *p*-cym), 5.73 (1H,m, =C*H*), 6.90 (4H, t, $^3J_{HH}$ = 7.2 Hz, BPh_4), 7.05 (8H, t, $^3J_{HH}$ = 7.2 Hz, BPh_4), 7.32 (8H, m, BPh_4), 7.12 – 7.80 (10H, m, PPh_2). $^{13}C\{^1H\}$ NMR (100.6 MHz, CD_2Cl_2, -30°C): δ 16.4 (m, Ru-CH_2), 17.0, 17.2 (2*s*, br, *Me*$_2$CH-P), 18.4 (s, Me), 21.1 (d, $^1J_{CP}$ = 15.6 Hz, Me$_2$*C*H-P), 21.5 (d, $^1J_{CP}$ = 14.4 Hz, Me$_2$*C*H-P), 21.9 (s, CH*Me*$_2$), 22.5 (d, $^1J_{CP}$ = 42.9 Hz, PCH_2-CH=), 22.6 (s, CH*Me*$_2$), 30.8 (s, *C*HMe$_2$), 32.3 (m, *C*HP), 33.4 (d, $^1J_{CP}$ = 31.7 Hz, Ru-PCH_2), 86.7, 87.2, 88.9, 89.3, 101.4, 109.8 (6*s*, *p*-cym) 121.9 (s, BPh_4), 124.2 (d, $^2J_{CP}$ = 8.0 Hz, =*C*H), 124.7 (d, $^3J_{CP}$ = 11.1 Hz, =*C*H$_2$), 125.8 (s, BPh_4), 128.3 – 133.7 (PPh_2), 135.8, (s, BPh_4), 164.0 (q, J_{C11B} = 50.3 Hz, BPh_4).

Synthesis of complex ($R_{Ru}S_C$/$S_{Ru}R_C$)-[RuCl(η^6-$C_{10}H_{14}$){κ^2*P,C*-$Ph_2PCH_2CH(Ph_2PCH_2CH=CH_2)CH_2$}][Cl]. To a solution of the complex [RuCl(μ-Cl)(η^6-$C_{10}H_{14}$)]$_2$ (0.1 g, 0.16 mmol) in methanol (10 mL), 5 equivalents of ADPP (0.8 mmol, 183 μL) were added. The resulting suspension was stirred for 2 hours at room temperature until solution is completed. After this time period, the solution was evaporated and the yellow residue was washed with diethyl ether (3 x 20 mL) and dried under reduced pressure. Spectroscopic data for complex [RuCl(η^6-$C_{10}H_{14}$){κ^2*P,C*-$Ph_2PCH_2CH(Ph_2PCH_2CH=CH_2)CH_2$}][Cl] are the same than for complex **6c** except for those signals due to the BPh_4 anion. Anal. Calcd for $C_{40}H_{44}Cl_2P_2Ru$: C, 63.3; H, 5.85. Found: C, 63.25; H, 5.8.

Synthesis of complex [RuCl(η^6-$C_{10}H_{14}$){κ^1*P*-$Ph_2PCH_2CH=CH_2$}(PPh_3)][BPh_4] (7). Method A: To a solution of the complex [RuCl(η^6-$C_{10}H_{14}$){κ^3*P,C,C*-$Ph_2PCH_2CH=CH_2$}][BPh_4] (**2**) (100 mg, 0.12 mmol) in THF (15 mL) 1 equivalent of PPh_3 (32 mg, 0.12 mmol) was added and the mixture was heated at reflux temperature for 30 minutes. The solution was then concentrated under vacuum to a volume of approx. 1 mL. Addition of hexane (30 mL) afforded a yellow precipitate. Solvents were decanted and the solid was washed with hexane (2 x 10 mL) and dried under reduced pressure. Yield: 78 mg, 60%. Method B: Complex [RuCl(η^6-$C_{10}H_{14}$){κ^2*(P,C)*-$Ph_2PCH_2CH(PPh_3)CH_2$}][BPh_4] (**6b**) (130 mg, 0.12 mmol) was refluxed in THF for 30 minutes. The solution was then concentrated to a volume of approx. 1 mL. and hexane (15 mL) was added. The yellow solid was washed with hexane (2 x 10 mL) and dried under reduced pressure. Yield: 69 mg, 53%. Anal. Calcd for $C_{67}H_{64}BClP_2Ru$: C, 74.6; H, 6.0. Found: C, 74.5; H, 6.1%. Conductivity (acetone, 20°C): Λ = 135 S cm^2 mol^{-1}. IR (KBr) ν_{max}/cm^{-1} 1579 (C=C), 733, 702 (BPh_4). $^{31}P\{^1H\}$ NMR (121.5 MHz, $CDCl_3$, 20°C): δ 19.5 (d, $^2J_{PP}$ = 52.2 Hz, PPh_3), 23.6 (d, $^2J_{PP}$ = 52.2 Hz, ADPP). ^1H NMR (400.1 MHz, $CDCl_3$, 20°C): δ 0.38 (3H, s, C-Me), 1.26 (6H, m, CH*Me*$_2$), 1.28 (1H, m, PCH_2), 2.74 (1H, sept, $^3J_{HH}$ = 6.8 Hz, C*H*Me$_2$), 3.15 (1H, m, PCH_2), 4.36 (1H, d, $^3J_{HH}$ = 16.8 Hz, =C*H*$_2$), 4.63 (1H, d, $^3J_{HH}$ = 10.4 Hz, =CH_2), 4.71 (1H, m, =CH), 4.83, 5.32 (2 x 2H, 2m, *p*-cym), 6.81 (4H, t, $^3J_{HH}$ = 7.2 Hz, BPh_4), 6.92 (8H, t, $^3J_{HH}$ = 7.2 Hz, BPh_4), 7.18 – 7.86 (45H, m, PPh_3, PPh_2, BPh_4). $^{13}C\{^1H\}$ NMR (100.6 MHz, $CDCl_3$, 20°C): δ 14.9 (s, Me), 21.1, 21.6 (2s, CH*Me*$_2$), 26.7 (d, $^1J_{CP}$ = 26.3 Hz, PCH_2), 31.7 (s, *C*HMe$_2$), 87.1 (d, $^2J_{CP}$ = 11.4 Hz, *p*-cym), 88.7 (d, $^2J_{CP}$ = 9.9 Hz, *p*-cym), 95.2, 99.2, 98.1, 115.2 (4*s*, *p*-cym), 120.5 (d, $^3J_{CP}$ = 9.9 Hz, =CH_2), 121.6, 125.4 (2s, BPh_4), 128.6 (d, $^2J_{CP}$ = 11.5 Hz, =CH), 129.0 – 134.5 (PPh_3, PPh_2), 136.2 (s, BPh_4), 164.1 (q, J_{C11B} = 50.3 Hz, BPh_4). MS-ESI (m/z): 759 (M^+, 100%), 497 (M – PPh_3, 23).

Synthesis of complexes ($R_{Ru}R_C$/$S_{Ru}S_C$)-[RuCl(η^6-$C_{10}H_{14}$){κ^2*(P,C)*-$Ph_2PCH_2CH(PR_3)CH_2$}][BPh_4] (PR_3 = PPh_3 (6b'), ADPP (6c')). A solution of the corresponding complex **6b** or **6c** (0.05 mmol) in THF was stirred at room temperature for 2 h (**6b**) or 7 days (**6c**). The solution was then concentrated under vacuum to a volume of approx. 1 mL. Addition of hexane (30 mL) afforded complexes **6b'** and **6c'** as a yellow precipitate. R = PPh_3 (**6b'**): Yield: 47 mg (87%). $^{31}P\{^1H\}$ NMR (121.5 MHz, CD_2Cl_2, 20°C): δ 66.6 (d, $^3J_{PP}$ = 74.1 Hz, Ru-PPh_2), 25.6 (d, $^3J_{PP}$ = 74.1 Hz, PPh_3). R = ADPP (**6c'**): Yield: 46 mg (89%). $^{31}P\{^1H\}$ NMR (162.1 MHz, $CDCl_3$, 20°C): δ 68.0 (d, $^3J_{PP}$ = 70.5 Hz, Ru-PPh_2), 27.4 (d, $^3J_{PP}$ = 70.5 Hz, CH-PPh_2). All the other analytical and spectroscopic data are the same as found for **6b** and **6c**, respectively.

X-Ray Crystal Structure Determination of Complexes 1, 3, 5a, 6a·CH_3OH, 6c' and 7. The most relevant crystal and refinement data are collected in Table S2 in the Supporting Information.

X-ray crystallographic data for **1**, **3**, **5a**, **6a** ·MeOH, **7** and **6c'** in CIF format (CCDC 1459032-1459037).

In all cases, diffraction data were recorded on an Oxford Diffraction Xcalibur Nova (Agilent) single crystal diffractometer, using Cu-Kα radiation (λ= 1.5418 Å). Images were collected at a 63 mm fixed crystal-detector distance, using the oscillation method, with 1° oscillation and variable exposure time per image. Data collection strategy was calculated with the program CrysAlis Pro CCD.[23] Data reduction and cell

refinement was performed with the program CrysAlis Pro RED.[23] An empirical absorption correction was applied using the SCALE3 ABSPACK algorithm as implemented in the program CrysAlis Pro RED.[23]

The software package WINGX[24] was used for space group determination, structure solution and refinement. The structures for **1** and **5a** were solved by Patterson interpretation and phase expansion using DIRDIF.[25] For complexes **3, 6a, 6c' and 7** the structures were solved by direct methods using SIR92.[26] In the crystal of **6a**·CH_3OH, one solvent molecule per unit formula of the complex is present. In **7**, solvent molecules in the structure were highly disordered and were impossible to refine using conventional discrete-atom models. To resolve these issues, the contribution of solvent electron density was removed by the SQUEEZE/PLATON.[27]

Isotropic least-squares refinement on F^2 using SHELXL2013[28] was performed. During the final stages of the refinements, all the positional parameters and the anisotropic temperature factors of all the non-H atoms were refined**.** The H atoms were geometrically placed riding on their parent atoms with isotropic displacement parameters set to 1.2 times the U_{eq} of the atoms to which they are attached (1.5 for methyl groups) (except for **1**, which the H atoms were found from different Fourier maps and included in a refinement with isotropic parameters).

The function minimized was $[\sum w(Fo^2 - Fc^2)/\sum w(Fo^2)]^{1/2}$ where $w = 1/[\sigma^2(Fo^2) + (aP)^2 + bP]$ (a and b values are collected in Table S2) with $\sigma(Fo^2)$ from counting statistics and $P = (Max(Fo^2, 0) + 2Fc^2)/3$.

Atomic scattering factors were taken from the International Tables for X-Ray Crystallography International.[29] The crystallographic plots were made with PLATON.[27]

Computational Methods. The structure of the two diastereoisomers of the complex cations $[RuCl(\eta^6\text{-}C_{10}H_{14})\{\kappa^2\textit{P,C-i}Pr_2PCH_2CH(PMe_3)CH_2\}]^+$ and $[RuCl(\eta^6\text{-}C_{10}H_{14})\{\kappa^2\textit{P,C-i}Pr_2PCH_2CH(iPr_2PCH_2CH{=}CH_2)CH_2\}]^+$ were investigated theoretically with the Density-functional Theory (DFT) method. The geometry of the two complexes was fully optimized with the B3LYP functional, using the 6-31G* basis set for C, H, P and Cl, and LANL2DZ for Ru. The stationary points located were characterized as minima by calculating the vibrational frequencies. The calculations were carried out with the program Gaussian09.[19]

Acknowledgements

This work was supported by the Spanish Ministerio de Educación y Ciencia (CTQ-2010-17005 and CTQ-2011-26481) and Consolider Ingenio 2010 (CSD2007-00006). I. G. de la Arada thanks the Spanish Ministerio de Educación Cultura y Deporte for a scholarship. We also thank J. González, Universidad de Oviedo, for the theoretical calculations on this paper and I. Merino from the SCTs of the Universidad de Oviedo for the low temperature NMR experiments.

Keywords: allylphosphanes • chelating phosphorus-carbon ligands • nucleophilic additions • *p*-cymene complexes • ruthenium(II) complexes

[1] a) A. Dasgupta, V. Ramkumar, S. Sankararaman, *RSC Advances* **2015**, *5*, 21558-21561; *b*) T. T. Adint, C. R. Landis, *J. Am. Chem. Soc.* **2014**, *136*, 7943-7953; *c*) C. Metallinos, L. Van Belle, *J. Organomet. Chem.* **2010,** *696*, 141-149.

[2] *a*) B. Ye, N. Cramer, *Acc. Chem. Res.* **2015**, *48*, 1308-1318; *b*) A. Linden, L. Llovera, J. Herrera, R. Dorta, G. Agrifoglio, R. Dorta *Organometallics* **2012**, *31*, 6162-6171; *c*) Y. Hiroi, N. Komine, M. Hirano, S. Komiya, *Organometallics* **2011**, *30*, 1307-1310; *d*) C. Defieber, H. Grützmacher, E. M. Carreira, *Angew. Chem. Int. Ed.* **2008**, *47*, 4482-4502.

[3] *a*) H. Brunner, M. Muschiol, T. Tsuno, H. Ike, T. Kurosawa, K. Koyama, *Angew. Chem. Int. Ed.* **2012**, *51*, 1067-1070; *b*) H. Brunner, M. Muschiol, T. Tsuno, H. Ike, T. Kurosawa, K. Koyama, M. Zabel, *Organometallics* **2011**, *30*, 3666-3676; *c*) L. Hintermann, L. Xiao, A. Labonne, U. Englert, *Organometallics* **2009**, *28*, 5739-5748; *d*) J. W. Faller, P. P. Fontaine, *Organometallics* **2007**, *26*, 1738-1743.

[4] *a*) J. L. McBee, T. D. Tilley, *Organometallics* **2010**, *29*, 184-192; *b*) C. Hahn, *Chem. Eur. J.* **2004**, *10*, 5888-5899.

[5] *a*) G. Lorusso, C. R. Barone, N. G. Di Masi, C. Pacifico, L. Maresca, G. Natile, *Eur. J. Inorg. Chem.* **2007**, 2144-2150.

[6] *a*) Z. Liu, H. Yamamichi, S. T. Madrahimov, J. F. Hartwig, *J. Am. Chem. Soc.* **2011**, *133*, 2772-2782; *b*) B. M. Cochran, *J. Am. Chem. Soc.* **2008**, *130*, 2786-2792.

[7] *a*) S. Martínez de Salinas, J. Díez, M. P. Gamasa, E. Lastra, *J. Organomet. Chem.* **2014**, *757*, 1-7; *b*) M. A. Esteruelas, A. M. López, S. Mozo, E. Oñate, *Organometallics* **2012**, *31*, 440-444; *c*) S. Clapham, P. Braunstein, N. M. Boag, R. Welter, M. J. Chetcuti, *Organometallics* **2008**, *27*, 1758-1764; *d*) J. Díez, M. P. Gamasa, J. Gimeno, E. Lastra, A. Villar, *Eur. J. Inorg. Chem.* **2006**, *1*, 78-87; *e*) M. Baya, M. L. Buil, M. A. Esteruelas, E. Oñate, *Organometallics* **2005**, *24*, 2030-2038; *f*) P. Álvarez, E. Lastra, J. Gimeno, P. Braña, J. A. Sordo, J. Gómez, L. R. Falvello, M. Bassetti, *Organometallics* **2004**, ***23***, 2956-2966; *g*) M. Bassetti, P. Álvarez, J. Gimeno, E. Lastra, *Organometallics* **2004**, *23*, 5127-5134; *h*) J. H. Nelson, K. Y. Ghebreyessus, *Synthesis and Reactivity in Inorganic and Metal-organic Chemistry* **2003**, *33*, 1329-1349; *i*) P. Álvarez, J. Gimeno, E. Lastra, S. García-Granda, J. F. Van der Maelen, M. Bassetti, *Organometallics* **2001**, *20*, 3762-3771.

[8] *a*) A. Villar, J. Díez, E. Lastra, M. P. Gamasa, *Organometallics* **2011**, *30*, 5803-5808; *b*) J. Díez, M. P. Gamasa, E. Lastra, A. Villar, E. Perez-Carreño, *Organometallics* **2007**, *26*, 5315-5322; *c*) J. Díez, M. P. Gamasa, J. Gimeno, E. Lastra, A. Villar, *J. Organomet. Chem.* **2006**, *691*, 4092-4099; *d*) J. Díez, M. P. Gamasa, J. Gimeno, E. Lastra, A. Villar, *Organometallics* **2005**, *24*, 1410-1418; *e*) P. Álvarez, E. Lastra, J. Gimeno, M. Bassetti, L. R. Falvello, *J. Am. Chem. Soc.* **2003**, *125*, 2386-2387.

[9] I. García de la Arada, J. Díez, M. P. Gamasa, E. Lastra, *Organometallics* **2013***, 32,* 4342-4352*.*

[10] $^{13}C\{^1H\}$ NMR spectrum of complex **2** could not be obtained due to the low solubility of the product in in CD_2Cl_2. Solutions of the complex in more polar solvents such as methanol or acetone led the complexes with the ADPP coordinated κ^1P.

[11] P. D. Smith, A. H. Wright, *J. Organomet. Chem.* **1998**, *559*, 141-147.

[12] K. Y. Ghebreyessus, J. H. Nelson, *Organometallics* **2000**, *19*, 3387-3392.

[13] A. Caballero, F. A. Jalon, B. R. Manzano, G. Espino, M. Pérez-Manrique, A. Mucientes, F. J. Poblete, M. Maestro *Organometallics* **2004**, *23*, 5694-5706.

[14] L. P. Barthel-Rosa, K. Maitra, J. Fischer, J. H. Nelson, *Inorg. Chem.* **1998**, *37*, 633-639.

[15] W. J. Geary, *Coord. Chem. Rev.* **1971**, *7*, 81-122.

[16] a) H. Mayr, A. R Ofial, *J. Phys. Org. Chem.* **2008**, *21*, 584; b) P. Jaramillo, P. Fuentealba, P. Pérez, *Chem. Phys. Lett.* **2006**, *427*, 421.

[17] Complexes $R_{Ru}S_C/S_{Ru}R_C$-$[RuCl(\eta^6\text{-}C_{10}H_{14})\{\kappa^2\textit{P,C-i}Pr_2PCH_2CH(PR_3)CH_2\}]^+$ (PR_3 = PPh_3 or ADPP) have been synthesized following the same procedures as for **6c** and **6d**, respectively. Experimental details for their synthesis and for the isomerization reactions can be found in the Supporting Information.

[18] I. Sánchez-Sordo, S. Martínez de Salinas, J. Díez, E. Lastra, M. P. Gamasa *Organometallics*, **2015**, *34*, 4581-4590.

[19] M. J. Frisch, G. W. Trucks, H. B. Schlegel, G. E. Scuseria, M. A. Robb, J. R. Cheeseman, G. Scalmani, V. Barone, B. Mennucci, G. A. Petersson, H. Nakatsuji, M. Caricato, X. Li, H. P. Hratchian, A. F. Izmaylov, J. Bloino, G. Zheng, J. L. Sonnenberg, M. Hada, M. Ehara, K. Toyota, R. Fukuda, J. Hasegawa, M. Ishida, T. Nakajima, Y. Honda, O. Kitao, H. Nakai, T. Vreven, J. A. Jr. Montgomery, J. E. Peralta, F. Ogliaro, M. Bearpark, J. J. Heyd, E. Brothers, K. N. Kudin, V. N. Staroverov, T. Keith, R. Kobayashi, J. Normand, K. Raghavachari, A. J. Rendell, C. Burant, S. S. Iyengar, J. Tomasi, M. Cossi, N. Rega, J. M. Millam, M. Klene, J. E. Knox, J. B. Cross, V. Bakken, C. Adamo, J. Jaramillo, R. Gomperts, R. E. Stratmann, O. Yazyev, A. J. Austin, R. Cammi, C. Pomelli, J. W. Ochterski, R. L. Martin, K. Morokuma, V. G. Zakrzewski, G. A. Voth, P. Salvador, J. J. Dannenberg, S. Dapprich, A. D. Daniels, O. Farkas, J. B. Foresman, J. V. Ortiz, J. Cioslowski, D. J. Fox, *Gaussian 09*, Revision B.01, Gaussian, Inc., Wallingford CT, **2010**.

[20] *a*) H. Maskill, *The Physical Basis of Organic Chemistry*; Oxford Science Publications, NY **1985**; *b*) G. S. Hammond, *J. Am. Chem. Soc*. **1955**, *77*, 334-338.

[21] M. A. Bennett, T. N. Huang, T. W. Matheson, A. K. Smith, *Inorg. Synth*. **1982**, *21*, 74-78.

[22] *P. Clark, J. L. S. Curtis, P. E. Garrou, G. E. Hartwell, Can. J. Chem.* **1974***,* 52¸ *1714–1720.*

[23] *CrysAlis*^{Pro} *CCD, CrysAlis*^{Pro} *RED. Oxford Diffraction Ltd., Abingdon, Oxfordshire, UK.* **2008***.*

[24] L. J. Farrugia, *J. Appl. Crystallogr.* **2012***, 45*, 849-854.

[25] P. T. Beurskens, G. Beurskens, R. de Gelder J. M. M, Smits S. García-Granda, R. O. Gould, C. Smykalla, *The DIRDIF Program System; Technical Report of the Crystallographic Laboratory*; University of Nijmegen: Nijmegen, The Netherlands, (**2008**). L. J Farrugia, Window GUI.

[26] A. Altomare, G. Cascarano, C. Giacovazzo, A. Guagliardi, M. C. Burla, G. Polidori, M. Camalli, *J. Appl. Cryst.* 1994, **27**, 435-436.

[27] A. L. Spek *PLATON: A Multipurpose Crystallographic Tool*; University of Utrecht, The Netherlands, **2007**.

[28] G. M. Sheldrick SHELXL2013 *Program for the Refinement of Crystal Structures*; University of Göttingen: Göttingen, Germany, **2014**.

[29] *Tables for X-Ray Crystallography*; Kynoch Press, Birminghan, U.K., **1974**; Vol. IV, present distributor: Kluwer Academic Publishers; Dordrecht, The Netherlands.

FULL PAPER

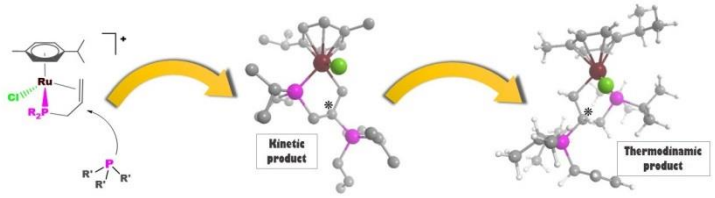

Diastereoselective

New ruthenium complexes containing bidentate κ^2*P,C*-ligands [RuCl(η^6-$C_{10}H_{14}$){κ^2*P,C*-$Ph_2PCH_2CH(PR_3)CH_2$}][BPh_4] have been diastereoselectively synthesized as the kinetically stable isomer ($R_{Ru}S_C/S_{Ru}R_C$). This diastereoisomer spontaneously evolves to the thermodynamically stable diastereoisomer ($R_{Ru}R_C/S_{Ru}S_C$). $^{31}P\{^1H\}$ NMR monitoring experiments shed light on the isomerization processes. DFT calculations agreee with the experimental results.

Diasteroselective addition

I. García de la Arada, J. Díez, M. P. Gamasa and E. Lastra.*

Page No. – Page No.

ISOMERIZATION PROCESSES ON ORGANORUTHENIUM COMPLEXES BEARING κ^2*P,C*- BIDENTATE LIGANDS GENERATED THROUGH NUCLEOPHILIC ADDITION TO COORDINATED ALKENYL PHOSPHANES